A Review of Water Hammer Theory and Practice

Mohamed S. Ghidaoui
email: ghidaoui@ust.hk

Ming Zhao
email: cezhm@ust.hk

Department of Civil Engineering, The Hong Kong
University of Science and Technology,
Hong Kong, China

Duncan A. McInnis
Surface Water Group, Komex International Ltd.,
4500 16th Avenue, Suite 100, N. W. Calgary,
Alberta T3B 0M6, Canada

David H. Axworthy
163 N. Marengo Avenue, #316, Pasadena,
CA 91101
email: bm300@lafn.org

Hydraulic transients in closed conduits have been a subject of both theoretical study and intense practical interest for more than one hundred years. While straightforward in terms of the one-dimensional nature of pipe networks, the full description of transient fluid flows pose interesting problems in fluid dynamics. For example, the response of the turbulence structure and strength to transient waves in pipes and the loss of flow axisymmetry in pipes due to hydrodynamic instabilities are currently not understood. Yet, such understanding is important for modeling energy dissipation and water quality in transient pipe flows. This paper presents an overview of both historic developments and present day research and practice in the field of hydraulic transients. In particular, the paper discusses mass and momentum equations for one-dimensional Flows, wavespeed, numerical solutions for one-dimensional problems, wall shear stress models; two-dimensional mass and momentum equations, turbulence models, numerical solutions for two-dimensional problems, boundary conditions, transient analysis software, and future practical and research needs in water hammer. The presentation emphasizes the assumptions and restrictions involved in various governing equations so as to illuminate the range of applicability as well as the limitations of these equations. Understanding the limitations of current models is essential for (i) interpreting their results, (ii) judging the reliability of the data obtained from them, (iii) minimizing misuse of water-hammer models in both research and practice, and (iv) delineating the contribution of physical processes from the contribution of numerical artifacts to the results of waterhammer models. There are 134 refrences cited in this review article. [DOI: 10.1115/1.1828050]

1 Introduction

Thus the growth of knowledge of the physical aspect of reality cannot be regarded as a cumulative process. The basic Gestalt of this knowledge changes from time to time . . . During the cumulative periods scientists behave as if reality is exactly as they know it except for missing details and improvements in accuracy. They speak of the laws of nature, for example, which are simply models that explain their experience of reality at a certain time. Later generations of scientists typically discover that these conceptions of reality embodied certain implicit assumptions and hypotheses that later on turned out to be incorrect. Vanderburg, [1]

Unsteady fluid flows have been studied since man first bent water to his will. The ancient Chinese, the Mayan Indians of Central America, the Mesopotamian civilizations bordering the Nile, Tigris, and Euphrates river systems, and many other societies throughout history have developed extensive systems for conveying water, primarily for purposes of irrigation, but also for domestic water supplies. The ancients understood and applied fluid flow principles within the context of ''traditional,'' culture-based technologies. With the arrival of the scientific age and the mathematical developments embodied in Newton's *Principia*, our understanding of fluid flow took a quantum leap in terms of its theoretical abstraction. That leap has propelled the entire development of hydraulic engineering right through to the mid-twentieth century. The advent of high-speed digital computers constituted another discrete transformation in the study and application of fluids engineering principles. Today, in hydraulics and other areas, engineers find that their mandate has taken on greater breadth and depth as technology rapidly enters an unprecedented stage of knowledge and information accumulation.

As cited in *The Structure of Scientific Revolutions*, Thomas Kuhn [2] calls such periods of radical and rapid change in our view of physical reality a ''revolutionary, noncumulative transition period'' and, while he was referring to scientific views of

reality, his remarks apply equally to our technological ability to deal with a revised or more complex view of the physical universe. It is in this condition that the field of closed conduit transient flow, and even more generally, the hydraulic analysis, design, and operation of pipeline systems, currently finds itself.

The computer age is still dawning, bringing with it a massive development and application of new knowledge and technology. Formerly accepted design methodologies, criteria, and standards are being challenged and, in some instances, outdated and revised. Computer aided analysis and design is one of the principal mechanisms bringing about these changes.

Computer analysis, computer modeling, and computer simulation are somewhat interchangeable terms, all describing techniques intended to improve our understanding of physical phenomena and our ability to predict and control these phenomena. By combining physical laws, mathematical abstraction, numerical procedures, logical constructs, and electronic data processing, these methods now permit the solution of problems of enormous complexity and scope.

This paper attempts to provide the reader with a general history and introduction to waterhammer phenomena, a general compendium of key developments and literature references as well as an updated view of the current state of the art, both with respect to theoretical advances of the last decade and modeling practice.

2 Mass and Momentum Equations for One-Dimensional Water Hammer Flows

Before delving into an account of mathematical developments related to waterhammer, it is instructive to briefly note the societal context that inspired the initial interest in waterhammer phenomena. In the late nineteenth century, Europe was on the cusp of the industrial revolution with growing urban populations and industries requiring electrical power for the new machines of production. As the fossil fuel era had not begun in earnest, hydroelectric generation was still the principal supply of this important energy source. Although hydroelectric generation accounts for a much smaller proportion of energy production today, the problems asso-

---

ciated with controlling the flow of water through penstocks and turbines remains an important application of transient analysis. Hydrogeneration companies contributed heavily to the development of fluids and turbomachinery laboratories that studied, among other things, the phenomenon of waterhammer and its control. Some of Allievi's early experiments were undertaken as a direct result of incidents and failures caused by overpressure due to rapid valve closure in northern Italian power plants. Frictionless approaches to transient phenomena were appropriate in these early developments because (i) transients were most influenced by the rapid closure and opening of valves, which generated the majority of the energy loss in these systems, and (ii) the pipes involved tended to have large diameters and the flow velocities tended to be small.

By the early 1900s, fuel oils were overtaking hydrogeneration as the principal energy source to meet society's burgeoning demand for power. However, the fascination with, and need to understand, transient phenomena has continued unabated to this day. Greater availability of energy led to rapid industrialization and urban development. Hydraulic transients are critical design factors in a large number of fluid systems from automotive fuel injection to water supply, transmission, and distribution systems. Today, long pipelines transporting fluids over great distances have become commonplace, and the almost universal development of sprawling systems of small pipe diameter, high-velocity water distribution systems has increased the importance of wall friction and energy losses, leading to the inclusion of friction in the governing equations. Mechanically sophisticated fluid control devices, including many types of pumps and valves, coupled with increasingly sophisticated electronic sensors and controls, provide the potential for complex system behavior. In addition, the recent knowledge that negative pressure phases of transients can result in contamination of potable water systems, mean that the need to understand and deal effectively with transient phenomena are more acute than ever.

2.1 Historical Development: A Brief Summary. The problem of water hammer was first studied by Menabrea [3] (although Michaud is generally accorded that distinction). Michaud [4] examined the use of air chambers and safety valves for controlling water hammer. Near the turn of the nineteenth century, researchers like Weston [5], Carpenter [6] and Frizell [7] attempted to develop expressions relating pressure and velocity changes in a pipe. Frizell [7] was successful in this endeavor and he also discussed the effects of branch lines, and reflected and successive waves on turbine speed regulation. Similar work by his contemporaries Joukowsky [8] and Allievi [9,10], however, attracted greater attention. Joukowsky [8] produced the best known equation in transient flow theory, so well known that it is often called the "fundamental equation of water hammer." He also studied wave reflections from an open branch, the use of air chambers and surge tanks, and spring type safety valves.

Joukowsky's fundamental equation of water hammer is as follows:

$$\Delta P = \pm \rho a \Delta V \quad \text{or} \quad \Delta H = \pm \frac{a \Delta V}{g} \tag{1}$$

where a = acoustic (waterhammer) wavespeed, $P = \rho g(H - Z)$ = piezometric pressure, Z = elevation of the pipe centerline from a given datum, H = piezometric head, ρ = fluid density, $V = \int_A u \, dA$ = cross-sectional average velocity, u = local longitudinal velocity, A = cross-sectional area of the pipe, and g = gravitational acceleration. The positive sign in Eq. (1) is applicable for a water-hammer wave moving downstream while the negative sign is applicable for a water-hammer wave moving upstream. Readers familiar with the gas dynamics literature will note that $\Delta P = \pm \rho a \Delta V$ is obtainable from the momentum jump condition under the special case where the flow velocity is negligible in comparison to the wavespeed. The jump conditions are a statement of the conserva-

tion laws across a jump (shock) [11]. These conditions are obtained either by directly applying the conservation laws for a control volume across the jump or by using the weak formulation of the conservation laws in differential form at the jump.

Allievi [9,10] developed a general theory of water hammer from first principles and showed that the convective term in the momentum equation was negligible. He introduced two important dimensionless parameters that are widely used to characterize pipelines and valve behavior. Allievi [9,10] also produced charts for pressure rise at a valve due to uniform valve closure. Further refinements to the governing equations of water hammer appeared in Jaeger [12,13], Wood [14], Rich [15,16], Parmakian [17], Streeter and Lai [18], and Streeter and Wylie [19]. Their combined efforts have resulted in the following classical mass and momentum equations for one-dimensional (1D) water-hammer flows

$$\frac{a^2}{g} \frac{\partial V}{\partial x} + \frac{\partial H}{\partial t} = 0 \tag{2}$$

$$\frac{\partial V}{\partial t} + g \frac{\partial H}{\partial x} + \frac{4}{\rho D} \tau_w = 0 \tag{3}$$

in which τ_w = shear stress at the pipe wall, D = pipe diameter, x = the spatial coordinate along the pipeline, and t = temporal coordinate. Although Eqs. (2) and (3) were fully established by the 1960s, these equations have since been analyzed, discussed, rederived and elucidated in numerous classical texts (e.g., [20–23]). Equations (2) and (3) constitute the fundamental equations for 1D water hammer problems and contain all the physics necessary to model wave propagation in complex pipe systems.

2.2 Discussion of the 1D Water Hammer Mass and Momentum Equations. In this section, the fundamental equations for 1D water hammer are derived. Special attention is given to the assumptions and restrictions involved in various governing equations so as to illuminate the range of applicability as well as the limitations of these equations.

Rapid flow disturbances, planned or accidental, induce spatial and temporal changes in the velocity (flow rate) and pressure (piezometric head) fields in pipe systems. Such transient flows are essentially unidirectional (i.e., axial) since the axial fluxes of mass, momentum, and energy are far greater than their radial counterparts. The research of Mitra and Rouleau [23] for the laminar water hammer case and of Vardy and Hwang [25] for turbulent water-hammer supports the validity of the unidirectional approach when studying water-hammer problems in pipe systems.

With the unidirectional assumption, the 1D classical water hammer equations governing the axial and temporal variations of the cross-sectional average of the field variables in transient pipe flows are derived by applying the principles of mass and momentum to a control volume. Note that only the key steps of the derivation are given here. A more detailed derivation can be found in Chaudhry [20], Wylie et al. [23], and Ghidaoui [26].

Using the Reynolds transport theorem, the mass conservation ("continuity equation") for a control volume is as follows (e.g., [20–23])
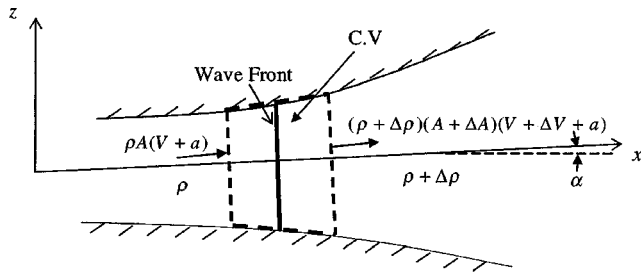
$$\frac{\partial}{\partial t} \int_{cv} \rho \, d\forall + \int_{cs} \rho (\mathbf{v} \cdot \mathbf{n}) dA = 0 \tag{4}$$

where cv = control volume, cs = control surface, $\mathbf{n}$ = unit outward normal vector to control surface, $\mathbf{v}$ = velocity vector.

Referring to Fig. 1, Eq. (4) yields

$$\frac{\partial}{\partial t} \int_x^{x+\delta x} \rho A \, dx + \int_{cs} \rho (\mathbf{v} \cdot \mathbf{n}) dA = 0 \tag{5}$$

The local form of Eq. (5), obtained by taking the limit as the length of the control volume shrinks to zero (i.e., δx tends to zero), is

Fig. 1 Control volume diagram used for continuity equation derivation

$$\frac{\partial(\rho A)}{\partial t} + \frac{\partial(\rho A V)}{\partial x} = 0 \tag{6}$$

Equation (6) provides the conservative form of the area-averaged mass balance equation for 1D unsteady and compressible fluids in a flexible pipe. The first and second terms on the left-hand side of Eq. (6) represent the local change of mass with time due to the combined effects of fluid compressibility and pipe elasticity and the instantaneous mass flux, respectively. Equation (6) can be rewritten as follows:

$$\frac{1}{\rho}\frac{D\rho}{Dt} + \frac{1}{A}\frac{DA}{Dt} + \frac{\partial V}{\partial x} = 0 \quad \text{or} \quad \frac{1}{\rho A}\frac{D\rho A}{Dt} + \frac{\partial V}{\partial x} = 0 \tag{7}$$

where $D/Dt = \partial/\partial t + V\partial/\partial x =$ substantial (material) derivative in one spatial dimension. Realizing that the density and pipe area vary with pressure and using the chain rule reduces Eq. (7) to the following:

$$\frac{1}{\rho}\frac{d\rho}{dP}\frac{DP}{Dt} + \frac{1}{A}\frac{dA}{dP}\frac{DP}{Dt} + \frac{\partial V}{\partial x} = 0 \quad \text{or} \quad \frac{1}{\rho a^2}\frac{DP}{Dt} + \frac{\partial V}{\partial x} = 0 \tag{8}$$

where $a^{-2} = d\rho/dP + (\rho/A)dA/dP$. The historical development and formulation of the acoustic wave speed in terms of fluid and pipe properties and the assumptions involved in the formulation are discussed in Sec. 3.

The momentum equation for a control volume is (e.g., [20–23]):

$$\sum F_{\text{ext}} = \frac{\partial}{\partial t}\int_{cv}\rho \mathbf{v}\forall + \int_{cs}\rho v(\mathbf{v}\cdot\mathbf{n})dA \tag{9}$$

Applying Eq. (9) to the control volume of Fig. 2; considering gravitational, wall shear and pressure gradient forces as externally applied; and taking the limit as δx tends to zero gives the following local form of the axial momentum equation:

$$\frac{\partial \rho A V}{\partial t} + \frac{\partial \beta \rho A V^2}{\partial x} = -A\frac{\partial P}{\partial x} - \pi D\tau_w - \gamma A \sin\alpha \tag{10}$$
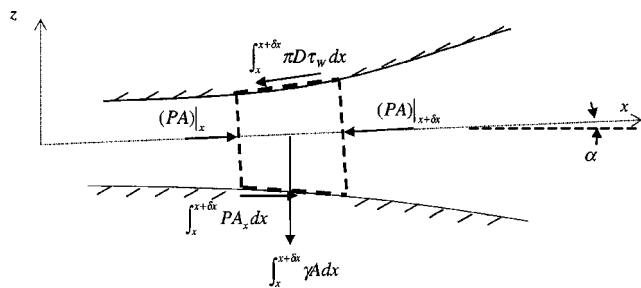
Fig. 2 Control volume diagram used for momentum equation derivation

where $\gamma = \rho \mathbf{g} =$ unit gravity force, $\alpha =$ angle between the pipe and the horizontal direction, $\beta = \int_A u^2 dA/V^2 =$ momentum correction coefficient. Using the product rule of differentiation, invoking Eq. (7), and dividing through by ρA gives the following nonconservative form of the momentum equation:

$$\frac{\partial V}{\partial t} + V\frac{\partial V}{\partial x} + \frac{1}{\rho A}\frac{\partial(\beta-1)\rho A V^2}{\partial x} + \frac{1}{\rho}\frac{\partial P}{\partial x} + \mathbf{g}\sin\alpha + \frac{\tau_w \pi D}{\rho A}$$
$$= 0 \tag{11}$$

Equations (8) and (11) govern unidirectional unsteady flow of a compressible fluid in a flexible tube. Alternative derivations of Eqs. (8) and (11) could have been performed by applying the unidirectional and axisymmetric assumptions to the compressible Navier-Stokes equations and integrating the resulting expression with respect to pipe cross-sectional area while allowing for this area to change with pressure.

In practice, the order of magnitude of water hammer wave speed ranges from 100 to 1400 m/s and the flow velocity is of order 1 to 10 m/s. Therefore, the Mach number, $\mathbf{M} = U_1/a$, in water-hammer applications is often in the range 10^{-2}–10^{-3}, where $U_1 =$ longitudinal velocity scale. The fact that $\mathbf{M} \ll 1$ in water hammer was recognized and used by Allievi [9,10] to further simplify Eqs. (8) and (11). The small Mach number approximation to Eqs. (8) and (11) can be illustrated by performing an order of magnitude analysis of the various terms in these equations. To this end, let $\rho_0 a U_1 =$ water hammer pressure scale, $\rho_0 =$ density of the fluid at the undisturbed state, and $T = \zeta L/a =$ time scale, where $L =$ pipe length, $X = aT = \zeta L =$ longitudinal length scale, $\zeta = a$ positive real parameter, $\rho f U_1^2/8 =$ wall shear scale, and $f = $ Darcy-Weisbach friction factor $T_d =$ radial diffusion time scale. The parameter ζ allows one to investigate the relative magnitude of the various terms in Eqs. (8) and (11) under different time scales. For example, if the order of magnitude of the various terms in the mass momentum over a full wave cycle (i.e., $T = 4L/a$) is desired, ζ is set to 4. Applying the above scaling to Eqs. (8) and (11) gives

$$\frac{\rho_0}{\rho}\frac{DP^*}{Dt^*} + \frac{\partial V^*}{\partial x^*} = 0 \quad \text{or}$$

$$\frac{\rho_0}{\rho}\left(\frac{\partial P^*}{\partial t^*} + \mathbf{M}V^*\frac{\partial P^*}{\partial x^*}\right) + \frac{\partial V^*}{\partial x^*} = 0 \tag{12}$$

$$\frac{\partial V^*}{\partial t^*} + \mathbf{M}V^*\frac{\partial V^*}{\partial x^*} + \mathbf{M}\frac{1}{\rho A}\frac{\partial(\beta-1)\rho A V^{*2}}{\partial x^*} + \frac{\rho_0}{\rho}\frac{\partial P^*}{\partial x^*}$$
$$+ \frac{\mathbf{g}\zeta L}{Ua}\sin\alpha + \frac{\zeta L}{D}\mathbf{M}\frac{f}{2}\tau_{w*} = 0 \tag{13}$$

where the superscript $*$ is used to denote dimensionless quantities. Since $\mathbf{M} \ll 1$ in water hammer applications, Eqs. (12) and (13) become

$$\frac{\rho_0}{\rho}\frac{\partial P^*}{\partial t^*} + \frac{\partial V^*}{\partial x^*} = 0 \tag{14}$$

$$\frac{\partial V^*}{\partial t^*} + \frac{\rho_0}{\rho}\frac{\partial P^*}{\partial x^*} + \frac{\mathbf{g}\zeta L}{Ua}\sin\alpha + \zeta\frac{L}{D}\mathbf{M}\frac{f}{2} + \zeta\left(\frac{T_d}{L/a}\right)\tau_{w*} = 0. \tag{15}$$

Rewriting Eqs. (14) and (15) in dimensional form gives

$$\frac{1}{\rho a^2}\frac{\partial P}{\partial t} + \frac{\partial V}{\partial x} = 0 \tag{16}$$

$$\frac{\partial V}{\partial t} + \frac{1}{\rho}\frac{\partial P}{\partial x} + \mathbf{g}\sin\alpha + \frac{\tau_w \pi D}{\rho A} = 0 \tag{17}$$

Using the Piezometric head definition (i.e., $P/\mathbf{g}\rho_0 = H - Z$), Eqs. (16) and (17) become

$$\frac{\mathbf{g}\rho_0}{\rho a^2}\frac{\partial H}{\partial t}+\frac{\partial V}{\partial x}=0 \tag{18}$$

$$\frac{\partial V}{\partial t}+\mathbf{g}\frac{\rho_0}{\rho}\frac{\partial H}{\partial x}+\frac{\tau_{\mathrm{w}}\pi D}{\rho A}=0 \tag{19}$$

The change in density in unsteady compressible flows is of the order of the Mach number [11,27,28]. Therefore, in water hammer problems, where $\mathbf{M}\ll1$, $\rho\approx\rho_0$, Eqs. (18) and (19) become

$$\frac{\mathbf{g}}{a^2}\frac{\partial H}{\partial t}+\frac{\partial V}{\partial x}=0 \tag{20}$$

$$\frac{\partial V}{\partial t}+\mathbf{g}\frac{\partial H}{\partial x}+\frac{\tau_{\mathrm{w}}\pi D}{\rho A}=0 \tag{21}$$

which are identical to the classical 1D water hammer equations given by Eqs. (2) and (3). Thus, the classical water hammer equations are valid for unidirectional and axisymmetric flow of a compressible fluid in a flexible pipe (tube), where the Mach number is very small.

According to Eq. (15), the importance of wall shear, τ_{w}, depends on the magnitude of the dimensionless parameter Γ $=\zeta L\mathbf{M}f/2D+\zeta T_d/(L/a)$. Therefore, the wall shear is important when the parameter Γ is order 1 or larger. This often occurs in applications where the simulation time far exceeds the first wave cycle (i.e., large ζ), the pipe is very long, the friction factor is significant, or the pipe diameter is very small. In addition, wall shear is important when the time scale of radial diffusion is larger than the wave travel time since the transient-induced large radial gradient of the velocity does not have sufficient time to relax. It is noted that T_d becomes smaller as the Reynolds number increases. The practical applications in which the wall shear is important and the various τ_w models that are in existence in the literature are discussed in Sec. 4.

If Γ is significantly smaller than 1, friction becomes negligible and τ_{w} can be safely set to zero. For example, for the case L $=10,000$ m, $D=0.2$ m, $f=0.01$, and $\mathbf{M}=0.001$, and $T_d/(L/a)$ $=0.01$ the condition $\Gamma\ll1$ is valid when $\zeta\ll4$. That is, for the case considered, wall friction is irrelevant as long as the simulation time is significantly smaller than $4L/a$. In general, the condition $\Gamma\ll1$ is satisfied during the early stages of the transient (i.e., ζ is small) provided that the relaxation (diffusion) time scale is smaller than the wave travel time L/a. In fact, it is well known that waterhammer models provide results that are in reasonable agreement with experimental data during the first wave cycle irrespective of the wall shear stress formula being used (e.g., [29–32]). When $\Gamma\ll1$, the classical waterhammer model, given by Eqs. (20) and (21), becomes

$$\frac{\mathbf{g}}{a^2}\frac{\partial H}{\partial t}+\frac{\partial V}{\partial x}=0 \tag{22}$$

$$\frac{\partial V}{\partial t}+\mathbf{g}\frac{\partial H}{\partial x}=0 \tag{23}$$

which is identical to the model that first appeared in Allievi [9,10].

The Joukowsky relation can be recovered from Eqs. (22) and (23). Consider a water hammer moving upstream in a pipe of length L. Let $x=L-at$ define the position of a water hammer front at time t and consider the interval $[L-at-\epsilon,L-at+\epsilon]$, where $\epsilon=$ distance from the water hammer front. Integrating Eqs. (22) and (23) from $x=L-at-\epsilon$ to $x=L-at+\epsilon$, invoking Leibnitz's rule, and taking the limit as ϵ approaches zero gives

$$\Delta H=-\frac{a\Delta V}{\mathbf{g}} \tag{24}$$

Similarly, the relation for a water hammer wave moving downstream is $\Delta H=+a\Delta V/\mathbf{g}$.

3 Water Hammer (Acoustic) Wave Speed

The water hammer wave speed is (e.g., [8,20,23,33,34]),

$$\frac{1}{a^2}=\frac{d\rho}{dP}+\frac{\rho}{A}\frac{dA}{dP} \tag{25}$$

The first term on the right-hand side of Eq. (25) represents the effect of fluid compressibility on the wave speed and the second term represents the effect of pipe flexibility on the wave speed. In fact, the wave speed in a compressible fluid within a rigid pipe is obtained by setting $dA/dP=0$ in Eq. (25), which leads to a^2 $=dP/d\rho$. On the other hand, the wave speed in an incompressible fluid within a flexible pipe is obtained by setting $d\rho/dP=0$ in (25), which leads to $a^2=AdP/\rho dA$.

Korteweg [33] related the right-hand side of Eq. (25) to the material and geometrical properties of the pipe. In particular, Korteweg [33] introduced the fluid properties through the state equation $dP/d\rho=K_f/\rho$, which was already well established in the literature, where $K_f=$ bulk modulus of elasticity of the fluid. He used the elastic theory of continuum mechanics to evaluate dA/dP in terms of the pipe radius, thickness e, and Young's modulus of elasticity E. In his derivation, he (i) ignored the axial (longitudinal) stresses in the pipe (i.e., neglected Poisson's effect) and (ii) ignored the inertia of the pipe. These assumptions are valid for fluid transmission lines that are anchored but with expansion joints throughout. With assumptions (i) and (ii), a quasi-equilibrium relation between the pressure force per unit length of pipe DdP and the circumferential (hoop) stress force per unit pipe length $2ed\sigma_\theta$ is achieved, where $\sigma_\theta=$ hoop stress. That is, $DdP=2ed\sigma_\theta$ or $dp=2ed\sigma_\theta/D$. Using the elastic stress-strain relation, $dA=\pi d\xi D^2/2$, where $d\xi$ $=d\sigma_\theta/E=$ radial (lateral) strain. As a result, $AdP/\rho dA=eE/D\rho$ and

$$\frac{1}{a^2}=\frac{\rho}{K_f}+\frac{\rho}{E\dfrac{e}{D}}\quad\text{or}\quad a^2=\frac{\dfrac{K_f}{\rho}}{1+\dfrac{K_fD}{eE}} \tag{26}$$

The above Korteweg formula for wave speed can be extended to problems where the axial stress cannot be neglected. This is accomplished through the inclusion of Poisson's effect in the stress-strain relations. In particular, the total strain becomes $d\xi$ $=d\sigma_\theta/E-\nu_{\mathrm{p}}d\sigma_x/E$, where $\nu_{\mathrm{p}}=$ Poisson's ratio and $\sigma_x=$ axial stress. The resulting wave speed formula is (e.g., [17,23])

$$a^2=\frac{\dfrac{K_f}{\rho}}{1+c\dfrac{K_fD}{eE}} \tag{27}$$

where $c=1-\nu_{\mathrm{p}}/2$ for a pipe anchored at its upstream end only, $c=1-\nu_{\mathrm{p}}^2$ for a pipe anchored throughout from axial movement, and $c=1$ for a pipe anchored with expansion joints throughout, which is the case considered by Korteweg (i.e., $\sigma_x=0$).

Multiphase and multicomponent water hammer flows are common in practice. During a water hammer event, the pressure can cycle between large positive values and negative values, the magnitudes of which are constrained at vapor pressure. Vapor cavities can form when the pressure drops to vapor pressure. In addition, gas cavities form when the pressure drops below the saturation pressure of dissolved gases. Transient flows in pressurized or surcharged pipes carrying sediment are examples of multicomponent water hammer flows. Unsteady flows in pressurized or surcharged sewers are typical examples of multiphase and multicomponent transient flows in closed conduits. Clearly, the bulk modulus and density of the mixture and, thus, the wave speed are influenced by the presence of phases and components. The wave speed for multiphase and multicomponent water hammer flows can be obtained
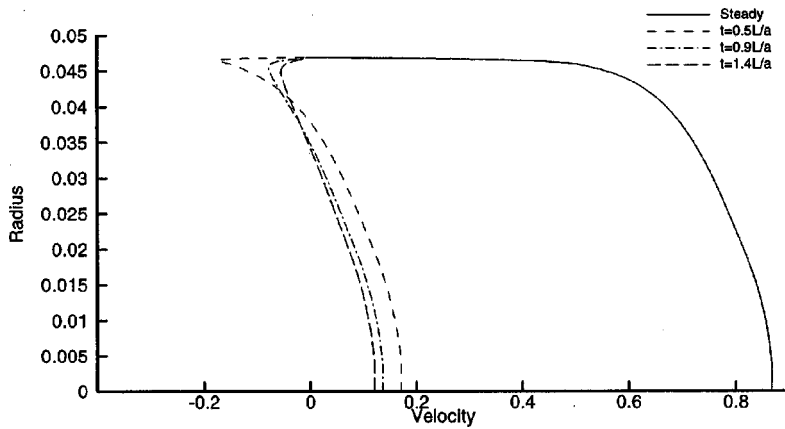
Fig. 3 Velocity profiles for steady-state and after wave passages

by substituting an effective bulk modulus of elasticity K_e and an effective density ρ_e in place of K_f and ρ in Eq. (27). The effective quantities, K_e and ρ_e, are obtained by the weighted average of the bulk modulus and density of each component, where the partial volumes are the weights (see, [23]). While the resulting mathematical expression is simple, the explicit evaluation of the wave speed of the mixture is hampered by the fact that the partial volumes are difficult to estimate in practice.

Equation (27) includes Poisson's effect but neglects the motion and inertia of the pipe. This is acceptable for rigidly anchored pipe systems such as buried pipes or pipes with high density and stiffness, to name only a few. Examples include major transmission pipelines like water distribution systems, natural gas lines, and pressurized and surcharged sewerage force mains. However, the motion and inertia of pipes can become important when pipes are inadequately restrained (e.g., unsupported, free-hanging pipes) or when the density and stiffness of the pipe is small. Some examples in which a pipe's motion and inertia may be significant include fuel injection systems in aircraft, cooling-water systems, unrestrained pipes with numerous elbows, and blood vessels. For these systems, a fully coupled fluid-structure interaction model needs to be considered. Such models are not discussed in this paper. The reader is instead directed to the recent excellent review of the subject by Tijsseling [35].

4 Wall Shear Stress Models

It was shown earlier in this paper that the wall shear stress term is important when the parameter Γ is large. It follows that the modeling of wall friction is essential for practical applications that warrant transient simulation well beyond the first wave cycle (i.e., large ζ). Examples include (i) the design and analysis of pipeline systems, (ii) the design and analysis of transient control devices, (iii) the modeling of transient-induced water quality problems, (iv) the design of safe and reliable field data programs for diagnostic and parameter identification purposes, (v) the application of transient models to invert field data for calibration and leakage detection, (vi) the modeling of column separation and vaporous cavitation and (vii) systems in which $L/a \ll T_d$. Careful modeling of wall shear is also important for long pipes and for pipes with high friction.

4.1 Quasi-Steady Wall Shear Models. In conventional transient analysis, it is assumed that phenomenological expressions relating wall shear to cross-sectionally averaged velocity in steady-state flows remain valid under unsteady conditions. That is, wall shear expressions, such as the Darcy-Weisbach and Hazen-Williams formulas, are assumed to hold at every instant during a transient. For example, the form of the Darcy-Weisbach equation used in water hammer models is (Streeter and Wylie [36])

$$\tau_w(t) = \tau_{ws} = \frac{\rho f(t)|V(t)|V(t)}{8} \tag{28}$$

where $\tau_{ws}(t) =$ quasi-steady wall shear as a function of t.

The use of steady-state wall shear relations in unsteady problems is satisfactory for very slow transients—so slow, in fact, that they do not properly belong to the water hammer regime. To help clarify the problems with this approach for fast transients, consider the case of a transient induced by an instantaneous and full closure of a valve at the downstream end of a pipe. As the wave travels upstream, the flow rate and the cross-sectionally averaged velocity behind the wave front are zero. Typical transient velocity profiles are given in Fig. 3. Therefore, using Eq. (28), the wall shear is zero. This is incorrect. The wave passage creates a flow reversal near the pipe wall. The combination of flow reversal with the no-slip condition at the pipe wall results in large wall shear stresses. Indeed, discrepancies between numerical results and experimental and field data are found whenever a steady-state based shear stress equation is used to model wall shear in water hammer problems (e.g., [25,30,32,37,38]).

Let $\tau_{wu}(t)$ be the discrepancy between the instantaneous wall shear stress $\tau_w(t)$ and the quasi-steady contribution of wall shear stress $\tau_{ws}(t)$. Mathematically

$$\tau_w(t) = \tau_{ws}(t) + \tau_{wu}(t) \tag{29}$$

$\tau_{wu}(t)$ is zero for steady flow, small for slow transients, and significant for fast transients. The unsteady friction component attempts to represent the transient-induced changes in the velocity profile, which often involve flow reversal and large gradients near the pipe wall. A summary of the various models for estimating $\tau_{wu}(t)$ in water hammer problems is given below.

4.2 Empirical-Based Corrections to Quasi-Steady Wall Shear Models. Daily et al. [39] conducted laboratory experiments and found $\tau_{wu}(t)$ to be positive for accelerating flows and negative for decelerating flows. They argued that during acceleration the central portion of the stream moved somewhat so that the velocity profile steepened, giving higher shear. For constant-diameter conduit, the relation given by Daily et al. [39] can be rewritten as

$$K_u = K_s + 2c_2 \frac{L}{V^2} \frac{\partial V}{\partial t} \tag{30}$$

where $K_u =$ unsteady flow coefficient of boundary resistance and momentum flux of absolute local velocity and $K_s = fL/D =$ steady state resistance coefficient. Daily et al. [39] noted that the longitudinal velocity and turbulence nonuniformities are negligible and $K_u \approx K = F/\rho A V^2/2 =$ unsteady flow coefficient of boundary resistance, where $F = 2\pi DL\tau_w =$ wall resistance force. Therefore, Eq. (30) becomes
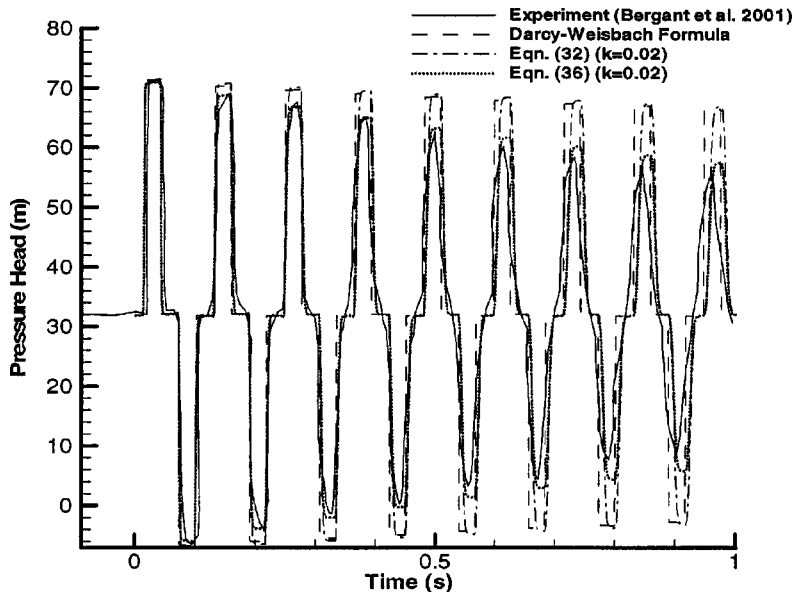
Fig. 4 Pressure head traces obtained from models and experiment

$$\tau_w = \frac{\rho f V^2}{8} + \frac{c_2 \rho D}{4} \frac{\partial V}{\partial t} \tag{31}$$

Denoting c_2 by k and $\rho f V^2/8$ by τ_{ws} reduces Eq. (31) to the following:

$$\tau_w = \tau_{ws} + \frac{k \rho D}{4} \frac{\partial V}{\partial t} \tag{32}$$

The formulations of Daily et al. [39] shows that coefficient $c_2 = k$ is a measure of the deviations, due to unsteadiness, of the wall shear and momentum flux. Therefore, k generally depends on x and t. This remark is supported by the extended thermodynamics approach used by Axworthy et al. [30]. Figure 4 clearly illustrates the poor agreement between model and data when using Eq. (32) with a constant value of k.

The experimental data of Daily et al. [39] show that $k = 0.01$ for accelerating flows and $k = 0.62$ for decelerating flows. On the other hand, the research of Shuy [40] led to $k = -0.0825$ for accelerating flows and $k = -0.13$ for decelerating flows. In fact, Shuy's data led him to conclude that unsteady wall friction increases in decelerating flows and decreases in accelerating flows. This result contradicts the previously accepted hypothesis, namely, that unsteady wall friction decreases in decelerating flows and increases in accelerating flows. Shuy [40] attributed the decrease in wall shear stress for acceleration to flow relaminarization. Given its controversial conclusion, this paper generated a flurry of discussion in the literature with the most notable remarks being those of Vardy and Brown [41].

Vardy and Brown [41] argued that Shuy's results should not be interpreted as contradicting previous measurements. Instead, the results indicated that the flow behavior observed in Shuy's experiments may have been different from the flow behavior in previous experiments. Vardy and Brown [41] put forward the time scale hypothesis as a possible explanation for the different flow behavior between Shuy's [40] experiments and previous ones. They also observed that, while Shuy's experiments dealt with long time scales, previous measurements dealt with much shorter time scales. Vardy and Brown [41] provided insightful and convincing arguments about the importance of time scale to the flow behavior in unsteady pipe flows. In fact, the stability analysis of Ghidaoui and Kolyshkin [42] concurs with the time scale hypothesis of Vardy and Brown [41]. Moreover, the stability analysis shows that, while other experiments belong to the stable domain, the experiments of Shuy belong to the unstable domain.

Theoretical investigations aimed at identifying the domain of applicability of Eq. (32) have appeared in the literature. For example, Carstens and Roller [43] showed that Eq. (32) can be derived by assuming that the unsteady velocity profiles obey the power law as follows:

$$\frac{u(x,r,t)}{V(x,t)} = \frac{(2n+1)(n+1)}{2n^2} \left(1 - \frac{r}{R}\right)^{1/n} \tag{33}$$

where $n = 7$ for Reynolds number $Re = 10^5$ and increases with Reynolds number, r = distance from the axis in a radial direction, R = radius of the pipe. An unsteady flow given by Eq. (33) describes flows that exhibit slow acceleration and does not allow for flow reversal (i.e., does not contain inflection points). In fact, Eq. (33) cannot represent typical water hammer velocity profiles such as those found in Vardy and Hwang [25], Silva-Araya and Chaudhry [37], Pezzinga [38,44], Eichinger and Lein [45] and Ghidaoui et al. [46]. The theoretical work of Carstens and Roller [43] shows only that Eq. (32) applies to very slow transients in which the unsteady velocity profile has the same shape as the steady velocity profile. Unfortunately, the Carstens and Roller [43] study neither supports nor refutes the possibility of using Eq. (32) in water hammer problems.

The theoretical work of Vardy and Brown [47] shows that Eq. (32) can be derived for the case of an unsteady pipe flow with constant acceleration. In addition, they show that this model is approximately valid for problems with time dependent acceleration as long as the time scale of the transient event greatly exceeds the rising time, which is a measure of time required for the vorticity diffusion through the shear layer. Their work also warns against using Eq. (32) for problems with time dependent acceleration induced by transient events with time scales smaller than the rising time (i.e., $L/a \ll T_d$).

Axworthy et al. [30] found that Eq. (32) is consistent with the theory of Extended Irreversible Thermodynamics (EIT) and satisfy the second law of thermodynamics. In addition, the EIT derivation shows that unsteady friction formulas based on instantaneous acceleration such as Eq. (32) are applicable to transient flow problems in which the time scale of interest (e.g., simulation time) is significantly shorter than the radial diffusion time scale of vorticity. Using the vorticity equation, Axworthy et al. [30] showed that for such short time scales, the turbulence strength and structure is unchanged (i.e., "frozen"), and the energy dissipation

behind a wave front is well represented by the degree of shift in the cross-sectional mean value of the velocity (i.e., dV/dt) and the cross-sectional mean value of V, itself.

The time scale arguments by Vardy and Brown [47] and Axworthy et al. [30] represent two limit cases: very slow transients and very fast transients, respectively. In the former case, there is enough mixing such that the acceleration history pattern is destroyed, only the instantaneous acceleration is significant to the wall shear stress. In the latter case, the pre-existing flow structure is frozen, there is no additional acceleration history developed except that of instantaneous acceleration. The Axworthy et al. [30] argument represents a water hammer flow situation where the acceleration behaves like a pulse, say, the flow drops from a finite value to zero in a short period.

An important modification of instantaneous acceleration-based unsteady friction models was proposed by Brunone and Golia [48], Greco [49], and Brunone et al. [50,51]. The well known Brunone et al. [50] model has become the most widely used modification in water hammer application due to its simplicity and its ability to produce reasonable agreement with experimental pressure head traces.

Brunone et al. [50] incorporated the Coriolis correction coefficient and the unsteady wall shear stress in the energy equation for water hammer as follows:

$$\frac{\partial H}{\partial x} + \frac{1}{\mathbf{g}}\frac{\partial V}{\partial t} + \frac{\eta + \phi}{\mathbf{g}}\frac{\partial V}{\partial t} + J_s = 0 \qquad (34)$$

where $\eta =$ difference from unity of the Coriolis correction coefficient, $J_s = (f|V|V)/2gD =$ steady-state friction term, $(\phi/\mathbf{g})(\partial V/\partial t) =$ difference between unsteady friction and its corresponding steady friction. In Eq. (34), the convective term is dropped as the Mach number of the flow is small in water hammer problems.

A constitutive equation is needed for $\eta + \phi$. Brunone et al. [50] proposed

$$\eta + \phi = k\left(1 - a\frac{\partial V}{\partial x} \bigg/ \frac{\partial V}{\partial t}\right) \qquad (35)$$

or in terms of wall shear stress

$$\tau_w = \tau_{ws} + \frac{k\rho D}{4}\left(\frac{\partial V}{\partial t} - a\frac{\partial V}{\partial x}\right) \qquad (36)$$

Equation (36) provides additional dissipation for a reservoir-pipe-valve system when the transient is caused by a downstream sudden valve closure. The pressure head traces obtained from the models and experiment are plotted in Fig. 4. It is shown that although both the Darcy-Weisbach formula and Eq. (32) with constant k cannot produce enough energy dissipation in the pressure head traces, the model by Brunone et al. [50] is quite successful in producing the necessary damping features of pressure peaks, verified by other researchers [29,52–55].

Slight modifications to the model of Brunone et al. [50], which renders this model applicable to both upstream and downstream transients, were proposed in [44] and in [52]. In particular, Pezzinga [44] proposed

$$\eta + \phi = k\left[1 + \text{sign}\left(V\frac{\partial V}{\partial x}\right)a\frac{\partial V}{\partial x} \bigg/ \frac{\partial V}{\partial t}\right] \qquad (37)$$

and Bergant et al. [53] proposed

$$\eta + \phi = k\left[1 + \text{sign}(V)a\left|\frac{\partial V}{\partial x}\right| \bigg/ \frac{\partial V}{\partial t}\right] \qquad (38)$$

The dependence of $\eta + \phi$ on x and t as well as the flow acceleration is consistent with the theoretical formulations in [30] and [39]. In addition, the form of $\eta + \phi$ gives significant correction for the unsteady friction when the flow is accelerated ($V\partial V/\partial t > 0$) and small correction when the flow is decelerated ($V\partial V/\partial t < 0$) [50].

Utilization of the models presented in this section requires a reliable estimate of the parameter k. The data of Brunone et al. [31], Daily et al. [39], and others show that k is not a universal constant. An empirical method for estimating this parameter was proposed by Brunone et al. [52] by fitting the decay of measured pressure head history. Moody diagram-like charts for k were developed by Pezzinga [44] using a quasi-two-dimensional turbulence model. Vardy and Brown [47] provided a theoretically-based expression for determining the coefficient k. This expression was successfully applied by Bergant et al. [52] and Vitkovsky et al. [55]. Although the charts of Pezzinga [44] and the formula of Vardy and Brown [47] are theory-based, their reliability is limited by the fact that they rely on steady-state-based turbulence models to adequately represent unsteady turbulence. It should, however, be stressed that modeling turbulent pipe transients is currently not well understood (see Sec. 9).

The mechanism that accounts for the dissipation of the pressure head is addressed in the discussion by Ghidaoui et al. [46]. They found that the additional dissipation associated with the instantaneous acceleration based unsteady friction model occurs only at the boundary due to the wave reflection. It was shown that after n_c complete wave cycles, the pressure head is damped by a factor equivalent to $[1/(1+k)]^{2n_c}$.

4.3 Physically Based Wall Shear Models. This class of unsteady wall shear stress models is based on the analytical solution of the unidirectional flow equations and was pioneered by Zielke [56]. Applying the Laplace transform to the axial component of the Navier-Stokes equations, he derived the following wall shear expression for unsteady laminar flow in a pipe:

$$\tau_w(t) = \frac{4\nu\rho}{R}V(t) + \frac{2\nu\rho}{R}\int_0^t \frac{\partial V}{\partial t'}(t')W(t-t')dt' \qquad (39)$$

where $t' =$ a dummy variable, physically represents the instantaneous time in the time history; $\nu =$ kinematic viscosity of the fluid; $W =$ weighting function

$$W(t) = e^{-26.3744(\nu t/R^2)} + e^{-70.8493(\nu t/R^2)} + e^{-135.0198(\nu t/R^2)}$$
$$+ e^{-218.9216(\nu t/R^2)} + e^{-322.5544(\nu t/R^2)}$$
$$\text{for} \quad \frac{\nu t}{R^2} > 0.02$$

$$W(t) = 0.282095\left(\frac{\nu t}{R^2}\right)^{-1/2} - 1.25000 + 1.057855\left(\frac{\nu t}{R^2}\right)^{1/2}$$
$$\text{for} \quad \frac{\nu t}{R^2} < 0.02 + 0.937500\frac{\nu t}{R^2} + 0.396696\left(\frac{\nu t}{R^2}\right)^{3/2}$$
$$- 0.351563\left(\frac{\nu t}{R^2}\right)^2 \qquad (40)$$

The first term on the right-hand side of Eq. (39) represents the steady-state wall shear stress τ_{ws} and the second term represents the correction part due to the unsteadiness of the flow τ_{wu}. The numerical integration of the convolution integral in Eq. (39) requires a large amount of memory space to store all previously calculated velocities and large central processing unit (CPU) time to carry out the numerical integration, especially when the time step is small and the simulation time large. Trikha [57] used three exponential terms to approximate the weighting function. The advantage of using exponential forms is that a recursive formula can easily be obtained, so that the flow history can be lumped into the quantities at the previous time step. In this way, only the calculated quantities at the previous time step needs to be stored in the computer memory, and there is no need to calculate the convolu-

tion integral from the beginning at every time step. This reduces the memory storage and the computational time greatly. In Suzuki et al. [58], for $\tau < 0.02$, the summation is calculated in a normal way; for $\tau > 0.02$, the recursive formula similar to that of Trikha [57] is used, since each of the five terms included in the weighting function is exponential. Although Zielke's formula is derived for laminar flow, Trikha [57] and others [29,52] found that this formula leads to acceptable results for low Reynolds number turbulent flows. However, Vardy and Brown [47] warned against the application of Zielke's formula outside the laminar flow regime, but did note that the error in applying Zielke's formula to turbulent flows diminishes as the duration of the wave pulse reduces.

Vardy et al. [59] extended Zielke's approach to low Reynolds number turbulent water hammer flows in smooth pipes. In a later paper, Vardy and Brown [60] developed an extension of the model of Vardy et al. [59] that was applicable to high Reynolds number transient flows in smooth pipes. In addition, Vardy and Brown [60] showed that this model gives results equivalent to those of Vardy et al. [59] for low Reynolds number flows and to those of Zielke [56] for laminar flows. That is, the Vardy and Brown [60] model promises to provide accurate results for Reynolds numbers ranging from the laminar regime to the highly turbulent regime. This model has the following form:

$$\tau_w(t) = \rho f \frac{V(t)|V(t)|}{8} + \frac{4\nu\rho}{D} \int_0^t W(t-t') \frac{\partial V}{\partial t'} dt' \quad (41)$$

where

$$W(t) = \alpha \exp(-\beta t)/\sqrt{\pi t}; \quad \alpha = D/4\sqrt{\nu};$$

$$\beta = 0.54\nu \, \text{Re}^\kappa/D^2; \quad \kappa = \log(14.3/\text{Re}^{0.05})$$

and Re=Reynolds number. Similar to Zielke's model, the convolution nature of Eq. (41) is computationally undesirable. An accurate, simple, and efficient approximation to the Vardy-Brown unsteady friction equation is derived and shown to be easily implemented within a 1D characteristics solution for unsteady pipe flow [32]. For comparison, the exact Vardy-Brown unsteady friction equation is used to model shear stresses in transient turbulent pipe flows and the resulting water hammer equations are solved by the method of characteristics. The approximate Vardy-Brown model is more computationally efficient (i.e., requires $\frac{1}{6}$-th the execution time and much less memory storage) than the exact Vardy-Brown model. Both models are compared with measured data from different research groups and with numerical data produced by a two-dimensional (2D) turbulence water hammer model. The results show that the exact Vardy-Brown model and the approximate Vardy-Brown model are in good agreement with both laboratory and numerical experiments over a wide range of Reynolds numbers and wave frequencies. The proposed approximate model only requires the storage of flow variables from a single time step while the exact Vardy-Brown model requires the storage of flow variables at all previous time steps and the 2D model requires the storage of flow variables at all radial nodes.

A summary of the assumptions involved in deriving Eqs. (39) and (41) is in order. The analytical approach of Zielke [56] involves the following assumptions: (i) the flow is fully developed, (ii) the convective terms are negligible, (iii) the incompressible version of the continuity equation is used (i.e., the influence of mass storage on velocity profile is negligible), and (iv) the velocity profile remains axisymmetric (i.e., stable) during the transient. In order to extend Zielke's approach to turbulent flows, Vardy and Brown [60] made two fundamental assumptions in relation to the turbulent eddy viscosity in addition to assumptions (i) through (iv). First, the turbulent kinematic viscosity is assumed to vary linearly within the wall shear layer and becomes infinite (i.e., a uniform velocity distribution) in the core region. Second, the turbulent eddy viscosity is assumed to be time invariant (i.e., frozen to its steady-state value). Assumptions (i), (ii), and (iii) are accurate for practical water hammer flows, where the Mach number is
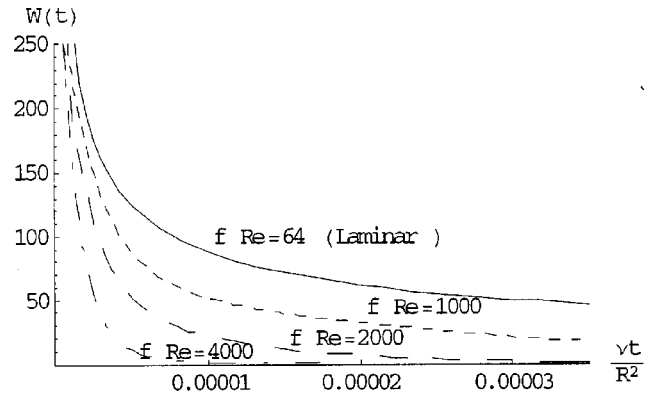

Fig. 5 Weighting function for different Reynolds numbers

often negligibly small and pipe length far exceeds flow development length. The validity of assumptions such as that the flow remains axisymmetric (stable), that the eddy viscosity is independent of time, and that its shape is similar to that in steady flow, is discussed later in the paper (see Secs. 6 and 7).

Understanding the connection between Eq. (32) and the physically based unsteady wall friction models proposed by Zielke [56] and Vardy and Brown [60] further illuminates the limitations of instantaneous acceleration, unsteady wall friction models as described in the previous section. In particular, it is evident from Eqs. (39) and (41) that Eq. (32) is recovered when the acceleration is constant. In addition, plots of W in Fig. 5 show that for flows with large Reynolds number, this function is very small everywhere except when $\nu t/R^2$ approaches 0, that is, when t' approaches t in Eq. (41). The region where $W(t-t')$ in Eq. (41) becomes significant and provides a measure of the time scale of the radial diffusion of vorticity T_d. If the acceleration varies slowly in the region where $W(t-t')$ is significant, it is clear that Eqs. (39) and (41) can be accurately approximated by Eq. (32). This is simply an alternative way to state that Eq. (32) is acceptable when the acceleration is not constant as long as the time scale of the flow disturbance far exceeds the time scale of radial diffusion of vorticity across the shear layer. Moreover, it is obvious that Eq. (32) is a good approximation to Eqs. (39) and (41) when t is small, as the integral interval is so small that the integrand can be considered as a constant. Furthermore, the time interval where $W(t-t')$ is significant reduces with Reynolds number, which shows that Eq. (32) becomes more accurate for highly turbulent flows.

5 Numerical Solutions for 1D Water Hammer Equations

The equations governing 1D water hammer (i.e., Eqs. (20) and (21)) can seldom be solved analytically. Therefore, numerical techniques are used to approximate the solution. The method of characteristics (MOC), which has the desirable attributes of accuracy, simplicity, numerical efficiency, and programming simplicity (e.g., [20,23,61]), is most popular. Other techniques that have also been applied to Eqs. (20) and (21) include the wave plan, finite difference (FD), and finite volume (FV) methods. Of the 11 commercially available water hammer software packages reviewed in Sec. 12, eight use MOC, two are based on implicit FD methods, and only one employs the wave-plan method.

5.1 MOC-Based Schemes. A significant development in the numerical solution of hyperbolic equations was published by Lister [62]. She compared the fixed-grid MOC scheme—also called the method of fixed time interval—with the MOC grid scheme and found that the fixed-grid MOC was much easier to compute, giving the analyst full control over the grid selection and enabling the computation of both the pressure and velocity fields

in space at constant time. Fixed-grid MOC has since been used with great success to calculate transient conditions in pipe systems and networks.

The fixed-grid MOC requires that a common time step (Δt) be used for the solution of the governing equations in all pipes. However, pipes in the system tend to have different lengths and sometimes wave speeds, making it impossible to satisfy the Courant condition (Courant number $C_r = a\Delta t/\Delta x \leqslant 1$) exactly if a common time step Δt is to be used. This discretization problem can be addressed by interpolation techniques, or artificial adjustment of the wave speed or a hybrid of both.

To deal with this discretization problem, Lister [62] used linear space-line interpolation to approximate heads and flows at the foot of each characteristic line. Trikha [57] suggested using different time steps for each pipe. This strategy makes it possible to use large time steps, resulting in shorter execution time and the avoidance of spatial interpolation error. This increased flexibility comes at the cost of having to interpolate at the boundaries, which can be a major source of error when complex, rapidly changing control actions are considered.

Wiggert and Sundquist [63] derived a single scheme that combines the classical space-line interpolation with reachout in space interpolation. Using Fourier analysis, they studied the effects of interpolation, spacing, and grid size on numerical dispersion, attenuation, and stability. These researchers found that the degree of interpolation ξ decreases as the ratio of the wavelength of the kth harmonic L_k to the reach length Δx increases. As a result, both numerical dissipation and dispersion are improved. These conclusions are not surprising for several reasons. First, every interpolation technique can be expected to produce better results for wave components with larger wavelengths. Second, for a fixed time step Δt, larger values of n imply smaller values of Δx and vice versa, since $n\Delta x$ represents the total length of the reachout on one side. Consequently, this scheme generates more grid points and, therefore, requires longer computational times and computer storage. Furthermore, an alternative scheme must be used to carry out the boundary computations.

The reachback time-line interpolation scheme, developed by Goldberg and Wylie [64], uses the solution from m previously calculated time levels. The authors observed that reachback time-line interpolation is more accurate than space-line interpolation for the same discretization. This is a subjective comparison because, as the degree of temporal interpolation ξ varies from 0 to 1, the degree of spatial interpolation α is only allowed to vary from $1/(m+1)$ to $1/m$. A fairer comparison would have been to also divide the distance step by m so that both ξ and α vary equally. In addition, Goldberg and Wylie [64] assert that numerical errors are reduced by increasing m. This is somewhat misleading because, for a fixed Δx, increasing m means increasing the number of computational steps (i.e., reducing the effective time step Δt) which in turn generates finer interpolation intervals. Moreover, in cases where the friction term is large and/or when the wave speed is not constant, reaching back in time increases the approximation error of these terms.

Lai [65] combined the implicit, temporal reachback, spatial reachback, spatial reachout, and the classical time and space-line interpolations into one technique called the multimode scheme. Depending on the choice of grid size ($\Delta t, \Delta x$) and the limit on the maximum allowable reachbacks in time m, this scheme may function as either of the methods or a combination of any two methods. Numerical errors were studied using a mass balance approach. Stability conditions were derived from Von Neumann analysis. The multimode scheme gives the user the flexibility to select the interpolation scheme that provides the best performance for a particular problem.

Yang and Hsu [66,67] published two papers dealing with the numerical solution of the dispersion equation in 1D and 2D, respectively. The authors propose reaching back in time more than one time step and then using the Holly-Preissmann method to interpolate either in space or in time. It is claimed that the reachback Holly-Preissmann scheme is superior to the classical Holly-Preissmann method. An interesting discussion of this work, published in Bentley [68], showed that the solution obtained by the classical Holly-Preissmann method when the time step equals $m\Delta t$ is identical to that obtained by the reachback in space Holly-Preissmann (i.e., the foot of the characteristic line is extended back more than one time step until it intersects the space-line) with m reachbacks and a time step value of Δt. The only difference is that the reachback approach produces $m-1$ extra intermediate solutions at the cost of more computational time.

Sibetheros et al. [69] showed that the spline technique is well suited to predicting transient conditions in simple pipelines subject to simple disturbances when the nature of the transient behavior of the system is known in advance. The most serious problem with the spline interpolation is the specification of the spline boundary conditions.

The authors point out that the selection procedure was a "trial and error" one involving many possibilities. This "flexibility" suffers from the curse of "permutability," i.e., in a complex system the number of permutations and combinations of spline boundary conditions can become enormous. Moreover, in many multipipe applications it is not accuracy that directly governs the selection of the time step, but the hydraulically shortest pipe in the system. Since the most successful spline boundary conditions necessarily involve several reaches, application of the method becomes problematic in short pipes. It would appear to require much smaller time steps simply to apply the method at all. Other necessary conditions for the success of spline schemes are: (i) the dependent variable(s) must be sufficiently smooth, (ii) the computation of the derivatives at internal nodes must be accurate, and (iii) the formulation of the numerical and/or physical derivative boundary conditions must be simple and accurate. Conditions (i) and (iii) are a problem in water hammer analysis because the boundary conditions are frequently nonlinear and complex, and the dependent variables may be discontinuous.

Karney and Ghidaoui [70] developed "hybrid" interpolation approaches that include interpolation along a secondary characteristic line, "minimum-point" interpolation (which reduces the distance from the interpolated point to the primary characteristic), and a method of "wave path adjustment" that distorts the path of propagation but does not directly change the wave speed. The resulting composite algorithm can be implemented as a preprocessor step and thus uses memory efficiently, executes quickly, and provides a flexible tool for investigating the importance of discretization errors in pipeline systems. The properties of the algorithm are analyzed theoretically and illustrated by example in the paper.

5.2 Other Schemes. The wave plan method [71] is similar to the MOC in the sense that both techniques explicitly incorporate wave paths in the solution procedure. However, the wave plan method requires that flow disturbance functions such as valve curves be approximated by piecewise constant functions. That is, flow disturbances are approximated by a series of instantaneous changes in flow conditions. The time interval between any two consecutive instantaneous changes in flow conditions is fixed. The piecewise constant approximation to disturbance functions implies that the accuracy of the scheme is first order in both space and time. Therefore, fine discretization is required for achieving accurate solutions to water hammer problems.

The wave plan method "lumps" friction at the center of each pipe. In particular, friction is modeled using a disturbance function, where the form of this function is determined using the "orifice analogy." This disturbance function is friction approximated by piecewise constant functions. The modeling of friction as a series of discrete disturbances in space and time generates small spurious waves. In general, with small values of friction, these would be observed only as low-amplitude noise on the main tran-

sient signal. It is also unclear as to how additional physics, such as convolution-integral unsteady friction models, can be incorporated with the wave plan methodology.

Wylie and Streeter [72] propose solving the water hammer equations in a network system using the implicit central difference method in order to permit large time steps. The resulting nonlinear difference equations are organized in a sparse matrix form and are solved using the Newton-Raphson procedure. Only pipe junction boundary conditions were considered in the case study. It is recognized that the limitation on the maximum time step is set by the frequency of the dependent variables at the boundaries. Two commercially available water hammer software packages use the four point implicit scheme (see Sec. 12 Water Hammer Software). The major advantage of implicit methods is that they are stable for large time steps (i.e., $C_r > 1$ [65,72]). Computationally, however, implicit schemes increase both the execution time and the storage requirement and need a dedicated matrix inversion solver since a large system of equations has to be solved. Moreover, for most problems, iterative schemes must also be invoked. From a mathematical perspective, implicit methods are not suitable for wave propagation problems because they entirely distort the path of propagation of information, thereby misrepresenting the mathematical model. In addition, a small time step is required for accuracy in water hammer problems in any case [23]. For these reasons, most of the work done on numerical modeling of hyperbolic equations in the last three decades concentrated on developing, testing, and comparing explicit schemes (e.g., [63,64,73]).

Chaudhry and Hussaini [74] apply the MacCormack, Lambda, and Gabutti schemes to the water hammer equations. These three methods are explicit, second-order (in time and space) finite difference schemes. Two types of boundary conditions are used: (i) one characteristic equation and one boundary equation, or (ii) extrapolation procedure boundary condition. The second boundary condition solution method adds one fictitious node upstream of the upstream boundary and another downstream of the downstream boundary. Using the L_1 and L_2 norms as indicators of the numerical errors, it was shown that these second-order finite-difference schemes produce better results than first-order method of characteristics solutions for $C_r = 0.8$ and 0.5. Spurious numerical oscillations are observed, however, in the wave profile.

Although FV methods are widely used in the solution of hyperbolic systems, for example, in gas dynamics and shallow water waves (see recent books by Toro [75,76]), this approach is seldom applied to water hammer flows. To the authors' knowledge, the first attempt to apply FV-based schemes was by Guinot [77]. He ignored the advective terms, developed a Riemann-type solution for the water hammer problem, and used this solution to develop a first-order-based FV Godunov scheme. This first-order scheme is very similar to the MOC with linear space-line interpolation. At the time of writing, a second paper by Hwang and Chung [78] that also uses the FV method for water hammer, has appeared. Unlike in Guinot [77], the advective terms are not neglected in the work of Hwang and Chung [78]. Instead, they use the conservative form of the compressible flow equations, in which density, and not head, is treated as an unknown. The application of such a scheme in practice would require a state equation relating density to head so that (i) all existing boundary conditions would have to be reformulated in terms of density and flow rather than head and flow, and (ii) the initial steady-state hydraulic grade line would need to be converted to a density curve as a function of longitudinal distance. At present, no such equation of state exists for water. Application of this method would be further complicated at boundaries where incompressible conditions are generally assumed to apply.

5.3 Methods for Evaluating Numerical Schemes. Several approaches have been developed to deal with the quantification of numerical dissipation and dispersion. The wide range of methods in the literature is indicative of the dissatisfaction and distrust among researchers of more conventional, existing techniques.

This section discusses a number of methods employed by transient modelers to quantify numerical dissipation and dispersion.

5.3.1 Von Neumann Method. Traditionally, fluid transient researchers have studied the dispersion and dissipation characteristics of the fixed-grid method of characteristics using the Von Neumann (or Fourier) method of analysis [63,64]. The Von Neumann analysis was used by O'Brian et al. [79] to study the stability of the numerical solution of partial differential equations. The analysis tracks a single Fourier mode with time and dissipation by determining how the mode decays with time. Dispersion is evaluated by investigating whether or not different Fourier modes travel with different speeds.

There are a number of serious drawbacks to the Von Neumann method of analysis. For example, it lacks essential boundary information, it ignores the influence of the wave profile on the numerical errors, it assumes constant coefficients and that the initial conditions are periodic, and it can only be applied to linear numerical models [69,79–81]. To illustrate, the work by Wiggert and Sundquist [63], Goldberg and Wylie [64], and others clearly shows that the attenuation and dispersion coefficients obtained from the Fourier analysis depend on the Courant number, the ratio of the wavelength of the kth harmonic L_k to the reach length Δx, and the number of reachbacks and/or reachouts, but does not depend on the boundary conditions. Yet, the simulation of boundary conditions and knowledge of how these boundary conditions introduce and reflect errors to the internal pipe sections is crucial to the study of numerical solutions of hydraulic problems. In short, the Von Neumann method cannot be used as the only benchmark for selecting the most appropriate numerical scheme for nonlinear boundary-value hyperbolic problems.

5.3.2 L_1 and L_2 Norms Method. Chaudhry and Hussaini [74] developed L_1 and L_2 norms to evaluate the numerical errors associated with the numerical solution of the water hammer equations by the MacCormack, Lambda, and Gabutti schemes. However, the L_1 and L_2 method as they apply it can only be used for problems that have a known, exact solution. In addition, these two norms do not measure a physical property such as mass or energy, thereby making the interpretation of the numerical values of these norms difficult. Hence, the L_1 and L_2 norms can be used to compare different schemes, but do not give a clear indication of how well a particular scheme performs.

5.3.3 Three Parameters Approach. Sibetheros et al. [69] used three dimensionless parameters to study various numerical errors. A discussion followed by Karney and Ghidaoui [82] and a closure was provided by the authors. Salient points from the discussion and closure are summarized below.

The attenuation parameter is intended to measure the numerical dissipation by different interpolation schemes by looking at the maximum head value at the valve. This parameter, however, underestimates the numerical attenuation because the computation of head and flow at the downstream end of the pipe uses one characteristic equation and one boundary equation. The dispersion parameter is intended to measure the numerical dispersion by different interpolation schemes. This parameter is determined by asserting that the change in the wave shape is governed by the constant diffusion equation with initial conditions described by the Heaviside function. Although this method allows a rudimentary comparison of simple system responses, general conclusions cannot be drawn for a hyperbolic equation based on a diffusion equation. The longitudinal displacement parameter is intended to measure the extent by which different numerical schemes artificially displace the wave front. However, this parameter only suggests to what degree the interpolation method used is symmetrically dispersive and says little about the magnitude of artificial displacement of the wave by the numerical scheme.

5.3.4 Mass Balance Approach. The mass balance method [83,84] is a more general technique than the other existing meth-

ods since this approach can be applied to a nonlinear transient problem with realistic boundary conditions. The basic idea is to check how closely a particular numerical method conserves mass. Note that the mass balance approach can become ineffective in cases where a numerical scheme conserves mass but not energy and momentum.

5.3.5 EHDE Approach. Ghidaoui and Karney [85] developed the concept of an equivalent hyperbolic differential equation (*EHDE*) to study how discretization errors arise in pipeline applications for the most common interpolation techniques used to deal with the discretization problem in fixed-grid MOC. In particular, it is shown that space-line interpolation and the Holly-Preissmann scheme are equivalent to a wave-diffusion model with an adjusted wave speed, but that the latter method has additional source and sink terms. Further, time-line interpolation is shown to be equivalent to a superposition of two waves with different wave speeds. The EHDE concept evaluates the consistency of the numerical scheme, provides a mathematical description of the numerical dissipation and dispersion, gives an independent way of determining the Courant condition, allows the comparison of alternative approaches, finds the wave path, and explains why higher-order methods should usually be avoided. This framework clearly points out that numerical approximation of the water hammer equations fundamentally changes the physical problem and must be viewed as a nontrivial transformation of the governing equations. For example, implicit methods, while noted for their stability characteristics, transform the water hammer problem into a superposition of wave problems, each of which has a wave speed different from the physical wave speed and at least one of which has an infinite wave speed. The infinite numerical wave speed associated with implicit schemes ensures that the numerical domain of dependence is larger than the physical domain of dependence, and explains why these are highly stable. While good for stability, the large discrepancy between the numerical and physical domains of dependence hinders the accuracy of these schemes. Another problem with implicit schemes is that they are often computationally inefficient because they require the inversion of large matrices.

5.3.6 Energy Approach. Ghidaoui et al. [86] developed an integrated energy approach for the fixed-grid MOC to study how the discretization errors associated with common interpolation schemes in pipeline applications arise and how these errors can be controlled. Specifically, energy expressions developed in this work demonstrate that both time-line and space-line interpolation attenuate the total energy in the system. Wave speed adjustment, on the other hand, preserves the total energy while distorting the partitioning of the energy between kinetic and internal forms. These analytic results are confirmed with numerical studies of several series pipe systems. Both the numerical experiments and the analytical energy expression show that the discretization errors are small and can be ignored as long as there is continuous work in the system. When the work is zero, however, a C_r value close to one is required if numerical dissipation is to be minimized. The energy approach is general and can be used to analyze other water hammer numerical schemes.

6 Flow Stability and the Axisymmetric Assumption

Existing transient pipe flow models are derived under the premise that no helical type vortices emerge (i.e., the flow remains stable and axisymmetric during a transient event). Recent experimental and theoretical works indicate that flow instabilities, in the form of helical vortices, can develop in transient flows. These instabilities lead to the breakdown of flow symmetry with respect to the pipe axis. For example, Das and Arakeri [87] performed unsteady pipe flow experiments where the initial flow was laminar and the transient event was generated by a piston. They found that when the Reynolds number and the transient time scale exceed a threshold value, the flow becomes unstable. In addition, they observed that the flow instability results in the formation of nonsta-

tionary helical vortices and that the breakdown of these vortices into turbulence is very rapid. The breakdown of the helical vortices into turbulence resulted in strong asymmetry in the flow with respect to the pipe axis. Brunone et al. [31,88] carried out measurements of water hammer velocity profiles in turbulent flows. They also observed strong flow asymmetry with respect to the pipe axis. In particular, they found that a short time after the wave passage, flow reversal no longer appears simultaneously in both the top and the bottom sides of the pipe. Instead, flow reversal appears to alternate between the bottom and top sides of the pipe. This is consistent with the asymmetry observed by Das and Arakeri [87]. The impact of instabilities on wall shear stress in unsteady pipe flows was measured by Lodahl et al. [89]. They found that inflectional flow instabilities induce fluctuations in the wall shear stress, where the root mean square of the wall shear stress fluctuation in the pipe was found to be as high as 45% of the maximum wall shear stress.

Das and Arakeri [87] applied linear stability analysis to unsteady plane channel flow to explain the experimentally observed instability in unsteady pipe flow. The linear stability and the experimental results are in good qualitative agreement. Ghidaoui and Kolyshkin [90] investigated the linear stability analysis of unsteady velocity profiles with reverse flow in a pipe subject to three-dimensional (3D) perturbation. They used the stability results to reinterpret the experimental results of Das and Arakeri [87] and assess their planar flow and quasi-steady assumptions. Comparison of the neutral stability curves computed with and without the planar channel assumption shows that this assumption is accurate when the ratio of the boundary layer thickness to the pipe radius is below 20%. Any point in the neutral stability curve represents the parameters combination such that the perturbations neither grow nor decay. Critical values for any of these parameters can be obtained from the neutral stability curve. For unsteady pipe flows, the parameters related are Re and t. Therefore, critical Re can be obtained.

The removal of the planar assumption not only improves the accuracy of stability calculations, but also allows for the flow stability of both axisymmetric and nonaxisymmetric modes to be investigated, and for the experimental results to be reinterpreted. For example, both the work of Ghidaoui and Kolyshkin [90] and the experiments of Das and Arakeri [87] show that the nonaxisymmetric mode is the least stable (i.e., the helical type).

With the aim of providing a theoretical basis for the emergence of helical instability in transient pipe flows, Ghidaoui and Kolyshkin [42] performed linear stability analysis of base flow velocity profiles for laminar and turbulent water hammer flows. These base flow velocity profiles are determined analytically, where the transient is generated by an instantaneous reduction in flow rate at the downstream end of a simple pipe system. The presence of inflection points in the base flow velocity profile and the large velocity gradient near the pipe wall are the sources of flow instability. The main parameters governing the stability behavior of transient flows are Reynolds number and dimensionless time scale. The stability of the base flow velocity profiles with respect to axisymmetric and asymmetric modes is studied and the results are plotted in the Reynolds number/time scale parameter space. It is found that the asymmetric mode with azimuthal wave number one is the least stable. In addition, it is found that the stability results of the laminar and the turbulent velocity profiles are consistent with published experimental data. The consistency between the stability analysis and the experiments provide further confirmation (i) that water hammer flows can become unstable, (ii) that the instability is asymmetric, (iii) that instabilities develop in a short (water hammer) time scale and, (iv) that Reynolds number and the wave time scale are important in the characterization of the stability of water hammer flows. Physically, flow instabilities change the structure and strength of the turbulence in a pipe, result in strong

flow asymmetry, and induce significant fluctuations in wall shear stress. These effects of flow instability are not represented in existing water hammer models.

In an attempt to gain an appreciation of the importance of including the effects of helical vortices in transient models, Ghidaoui et al. [46] applied current transient models to flow cases with and without helical vortices. In the case where stability results indicate that there are no helical vortices, Ghidaoui et al. [46] found that the difference between water hammer models and the data of Pezzinga and Scandura [91] increases with time at a mild rate. However, for the case where stability results and experiments indicate the presence of helical vortices, it is found that the difference between water hammer models and the data of Brunone et al. [31] exhibits an exponential-like growth. In fact, the difference between models and the data of Brunone et al. [31] reaches 100% after only six wave cycles. This marked difference between models and data suggests that the influence of helical vortices on the flow field is significant and cannot be neglected.

7 Quasi-Steady and Frozen Turbulence Assumptions

The convolution integral analytical models for wall shear in unsteady turbulent flows derived in Vardy et al. [59] and Vardy and Brown [60] assume that eddy viscosity remains "frozen" (i.e., time independent) during the transient. Turbulence closure equations used by Vardy and Hwang [25], Silva-Araya and Chaudhry [37], and Pezzinga [38] assume that the turbulence changes in a quasi-steady manner and that the eddy viscosity expressions derived for steady-state pipe flows remain applicable for water hammer flows. An understanding of the response of the turbulence field to water hammer waves is central to judging the accuracy of using either the frozen or the quasi-steady turbulence assumptions.

There is a time lag between the passage of a wave front at a particular location along the pipe and the resulting change in turbulent conditions at this location (e.g., [46,92,93]). In particular, at the instant when a water hammer wave passes a position x along the pipe, the velocity field at x undergoes a uniform shift (i.e., the fluid exhibits a slug flowlike motion). The uniform shift in velocity field implies that the velocity gradient and turbulent conditions are unaltered at the instant of the wave passage. However, the combination of the uniform shift in velocity with the no-slip condition generates a vortex sheet at the pipe wall. The subsequent diffusion of this vortex ring from the pipe wall to the pipe core is the mechanism responsible for changing the turbulence conditions in the pipe.

A short time after the wave passage, the extent of vorticity diffusion is limited to a narrow wall region and the turbulence field is essentially frozen. In this case, both the quasi-steady turbulence and "frozen" turbulence assumptions are equally applicable. A similar conclusion was reached by Greenblatt and Moss [92] for a temporally accelerating flow; by Tu and Ramparian [94], Brereton et al. [95], and Akhavan et al. [96,97] for oscillatory flow; He and Jackson [93] for ramp-type transients; and Ghidaoui et al. [46] for water hammer flows. As the time after the wave passage increases, the extent of the radial diffusion of vorticity becomes more significant and begins to influence the velocity gradient and turbulence strength and structure in the buffer zone. The experiments of He and Jackson [93] show that the axial turbulent fluctuations are the first to respond to the changes in the radial gradient of the velocity profile and that there is a time delay between the changes in the axial turbulent fluctuations and its redistribution among the radial and azimuthal turbulent components. The production of axial turbulent kinetic energy and the time lag between production and redistribution of axial turbulent kinetic energy within the buffer zone are not incorporated in steady-state-based turbulence models. The characteristics of the flow in the core region will start to change only when the wave-induced shear pulse emerges from the buffer zone into the core region. On the basis of their unsteady flow experiments, He and

Jackson [93] provided an estimate for the time delay from the moment the wall vortex ring was generated at the pipe wall to the moment when significant changes in the structure and strength of turbulence appeared near the pipe axis.

Ghidaoui et al. [46] proposed a dimensionless parameter P for assessing the accuracy of quasi-steady turbulence modeling in water hammer problems. This parameter is defined as the ratio of the time scale of radial diffusion of vorticity to the pipe core to the time scale of wave propagation from one end of the pipe to the other. This parameter provides a measure for the number of times a wave front travels from one end of the pipe to the other before the preexisting turbulence conditions start to respond to the transient event. It follows that the frozen and quasi-steady assumptions are (i) acceptable when $P \gg 1$, (ii) questionable when P is of order 1, and (iii) applicable when $P \ll 1$. However, the last case does not belong to the water hammer regime. These conclusions are supported by the work of Ghidaoui et al. [46], where they compared the results of quasi-steady turbulence models with available data and by the work of Ghidaoui and Mansour [32] where they compared the results of frozen eddy viscosity models with experimental data.

8 Two-Dimensional Mass and Momentum Equations

Quasi-two-dimensional water hammer simulation using turbulence models can (i) enhance the current state of understanding of energy dissipation in transient pipe flow, (ii) provide detailed information about transport and turbulent mixing (important for conducting transient-related water quality modeling), and (iii) provide data needed to assess the validity of 1D water hammer models. Examples of turbulence models for water hammer problems, their applicability, and their limitations can be found in Vardy and Hwang [25], Silva-Araya and Chaudhry [37,98], Pezzinga [38,44], Eichinger and Lein [45], Ghidaoui et al. [46], and Ohmi et al. [99]. The governing equations for quasi-two-dimensional modeling are discussed in this section. Turbulence models and numerical solutions are presented in subsequent sections.

The most widely used quasi-two-dimensional governing equations were developed by Vardy and Hwang [25], Ohmi et al. [99], Wood and Funk [100], and Bratland [101]. Although these equations were developed using different approaches and are written in different forms, they can be expressed as the following pair of continuity and momentum equations:

$$\frac{\mathbf{g}}{a^2}\left(\frac{\partial H}{\partial t} + u\frac{\partial H}{\partial x}\right) + \frac{\partial u}{\partial x} + \frac{1}{r}\frac{\partial rv}{\partial r} = 0 \qquad (42)$$

$$\frac{\partial u}{\partial t} + u\frac{\partial u}{\partial x} + v\frac{\partial u}{\partial r} = -\mathbf{g}\frac{\partial H}{\partial x} + \frac{1}{r\rho}\frac{\partial r\tau}{\partial r} \qquad (43)$$

where x, t, u, H, r are defined as before, $v(x,r,t)$ = local radial velocity, and τ = shear stress. In this set of equations, compressibility is only considered in the continuity equation. Radial momentum is neglected by assuming that $\partial H/\partial r = 0$, and these equations are, therefore, only quasi-two-dimensional. The shear stress τ can be expressed as

$$\tau = \rho \nu \frac{\partial u}{\partial r} - \rho \overline{u'v'} \qquad (44)$$

where u' and v' = turbulence perturbations corresponding to longitudinal velocity u and radial velocity v, respectively. Turbulence models are needed to describe the perturbation term $-\rho \overline{u'v'}$ since most practical water hammer flows are turbulent.

The governing equations can be further simplified by neglecting nonlinear convective terms, as is done in the 1D case since the wave speed a is usually much larger than the flow velocity u or v. Then the equations become the following:

$$\frac{\mathbf{g}}{a^2}\frac{\partial H}{\partial t} + \frac{\partial u}{\partial x} + \frac{1}{r}\frac{\partial rv}{\partial r} = 0 \qquad (45)$$

$$\frac{\partial u}{\partial t} + \mathbf{g}\frac{\partial H}{\partial x} = \frac{1}{r\rho}\frac{\partial r\tau}{\partial r} \tag{46}$$

These governing equations are usually solved by numerical means.

For an adequately anchored or restrained pipe, i.e., the pipe is rigid and the radial velocity at the pipe wall is zero. From flow symmetry, the radial velocity at the centerline is also zero. Integrating Eq. (45) across the pipe section, the radial velocity vanishes, leaving the following:

$$\frac{\partial H}{\partial t} + \frac{a^2}{\mathbf{g}A}\frac{\partial Q}{\partial x} = 0 \tag{47}$$

$$\frac{\partial u}{\partial t} + \mathbf{g}\frac{\partial H}{\partial x} = \frac{1}{r\rho}\frac{\partial r\tau}{\partial r} \tag{48}$$

$$Q(x,t) = \int_A u\, dA \tag{49}$$

where $Q=$ discharge. These equations are the same as those presented by Pezzinga [38].

In cases where the radial velocity component (mass flux) is negligible, Eqs. (47)–(49) can be usefully applied. However, the inclusion of radial fluxes in Eqs. (45) and (46) remove the inconsistency that occurs near boundary elements due to the simultaneous imposition of the no-slip condition and the plane wave assumption [24]. Since numerical integration of Eq. (49) is needed to relate velocity distribution to discharge, even very small errors from neglecting radial fluxes can produce spurious oscillations in pressure head calculations.

Ghidaoui [26] derived quasi-two-dimensional equations from the complete 3D continuity equation and Navier-Stokes equations using an ensemble averaging process in which the assumptions inherent in the quasi-two-dimensional equations (such as flow axisymmetry and the plane wave assumption) are made explicit. The scaling analysis [26] shows that the viscous terms associated with the compressibility of the fluid are significantly smaller than the viscous term associated with angular deformation. Therefore, the compressibility is neglected in the momentum equations of both 1D and 2D models.

In Silva-Araya and Chaudhry [37,98] and Eichinger and Lein [45], an integration of the momentum equation is also carried out. In each case, the system reduces to a 1D formulation. The quasi-two-dimensional momentum Eq. (46) is only used to provide an unsteady friction correction for 1D governing equations. These corrections include: (i) an energy dissipation factor, which is the ratio of the energy dissipation calculated from the cross-sectional velocity distribution to that calculated from the Darcy-Weisbach formula [37,98] or (ii) direct calculation of wall shear stress, either by velocity gradient at the pipe wall or through energy dissipation [45].

9 Turbulence Models

Turbulence models are needed to estimate the turbulent perturbation term for $-\rho\overline{u'v'}$. In the water hammer literature, the widely used turbulence models are algebraic models [25,37,38,98,99] in which eddy viscosity is expressed as some algebraic function of the mean flow field. Other sophisticated models (such as the $k-\epsilon$ model, which require additional differential equations for eddy viscosity) have also been tried [45]. Similar results for the pressure head traces have been obtained.

The algebraic turbulence models used by Vardy and Hwang [25] and Pezzinga [38] are discussed further to illustrate some features of algebraic turbulence models. These models were comparatively studied by Ghidaoui et al. [46]. The comparison shows that very similar dissipation is produced by the two models. Other different variations of algebraic turbulence models are available in Rodi [102].

9.1 Five-Region Turbulence Model. The model used by Vardy and Hwang [25] is a direct extension of the model developed by Kita et al. [103] for steady flow

$$\tau = \rho(\nu + \epsilon)\frac{\partial u}{\partial r} = \rho\nu_T\frac{\partial u}{\partial r} \tag{50}$$

where $\epsilon=$ eddy viscosity, $\nu_T=$ total viscosity, and the other terms were previously defined. The total viscosity distribution is compartmentalized into five regions as follows:

1. viscous layer $\quad\dfrac{\nu_T}{\nu}=1\quad 0\leqslant y_*\leqslant\dfrac{1}{a}$ $\hfill(51)$

2. buffer I layer $\quad\dfrac{\nu_T}{\nu}=ay_*\quad \dfrac{1}{a}\leqslant y_*\leqslant\dfrac{a}{C_B}$ $\hfill(52)$

3. buffer II layer $\quad\dfrac{\nu_T}{\nu}=C_By_*^2$

$$\frac{a}{C_B}\leqslant y_*\leqslant\frac{\kappa}{C_B+\kappa^2/4C_mR_*} \tag{53}$$

4. logarithmic region $\quad\dfrac{\nu_T}{\nu}=\kappa y_*[1-(\kappa/4C_m)(y_*/R_*)]$

$$\times\frac{\kappa}{C_B+\kappa^2/4C_mR_*}$$

$$\leqslant y_*\leqslant\frac{1}{\kappa}2C_m(1+\sqrt{1-C_c/C_m})R_* \tag{54}$$

5. core region $\quad\dfrac{\nu_T}{\nu}=C_cR_*\quad \dfrac{1}{\kappa}2C_m(1+\sqrt{1-C_c/C_m})R_*\leqslant y_*$

$$\leqslant R_* \tag{55}$$

where $y=R-r$, $y_*=u_*y/\nu$, $R_*=u_*R/\nu$, $u_*=\sqrt{\tau_w/\rho}$, and the coefficients are $a=0.19$, $C_B=0.011$, $\kappa=0.41$, $C_m=0.077$, and $C_c=$ a function of Reynolds number (usually a value of 0.06 is used). The total viscosity distribution depends on friction velocity u_* and position y only. This is true for steady flow since all information at interior points will ultimately propagate to the wall boundary. Given sufficient time, the velocity profile adjusts and finally depends on wall shear stress only. However, this model may be problematic for unsteady flow since the interior conditions cannot solely be represented by wall shear stress.

9.2 Two-Layer Turbulence Model. In the two-layer turbulence model, flow is divided into two layers: (i) a smooth pipe, viscous sublayer is assumed to exist near the wall; and (ii) outside the viscous sublayer, the Prandtl mixing length hypothesis is used

1. viscous sublayer $\quad\epsilon=0\quad y_*\leqslant 11.63$ $\hfill(56)$

2. turbulent region $\quad\epsilon=l^2\left|\dfrac{\partial u}{\partial r}\right|\quad y_*\geqslant 11.63$ $\hfill(57)$

where

$$\frac{l}{R}=\kappa\frac{y}{R}e^{-(y/R)} \tag{58}$$

$$\kappa=0.374+0.0132\ln\left(1+\frac{83100}{\text{Re}}\right) \tag{59}$$

and in which $l=$ mixing length and Re$=$ Reynolds number for initial flow. The thickness of the viscous sublayer is determined by the wall shear stress. The eddy viscosity in the turbulent region includes some information about the velocity profile. The two-layer model appears to be more suitable for unsteady flow simu-

lation, but one should note that the expression for mixing length and the empirical coefficient κ are based on steady flow equivalents.

Ghidaoui et al. [46] compared both models (i.e., the five-region and the two-layer model) and obtained very similar results for pressure head estimates. The comparative study suggests that the pressure head is not sensitive to eddy viscosity distribution in the pipe core region. As these models are based on steady flow principles, the application of these models to unsteady flow problems implicitly includes the quasi-steady assumptions discussed in Section 7.

These algebraic turbulence models are widely used, mainly because of their simplicity and robustness. As more powerful computers become available and improvements are made to numerical solution techniques, detailed turbulence structures may be obtained using more sophisticated turbulence models, such as the two-equation $k-\epsilon$ models, or perhaps even Reynolds stress models, for which no eddy viscosity hypothesis is needed.

All of the models mentioned above are based on the Reynolds-averaged Navier-Stokes (RANS) equation. The averaging process is clearly a time average and valid for steady flows. For unsteady flows, the use of the time average is highly questionable unless the unsteadiness has a much larger time scale than the time scale of turbulence. Obviously, this is not the case for fast transients.

As an alternative, large eddy simulation (LES) has been developed recently. In LES, the Navier-Stokes equation is filtered, large-scale motion is resolved while the small-scale motion is modeled. If results from LES were available, then some of the assumptions mentioned previously could, in principle, be more rigorously evaluated. Unfortunately, in carrying out LES, a full 3D system of equations must be solved using very fine grids [104]. For steady flow simulations, when the turbulence statistics reach steady, the ensemble average can be obtained over a time interval from a single run [104]. However, the ensemble average cannot be obtained from a single run for transient flow. The requirement of many runs makes the resulting computational process prohibitively time consuming. As yet, such analyses have not been performed in pipe transients.

10 Numerical Solution for 2D Problems

The 2D governing equations are a system of hyperbolic-parabolic partial differential equations. The numerical solution of

Vardy and Hwang [25] solves the hyperbolic part of governing equations by MOC and the parabolic part using finite difference. This hybrid solution approach has several merits. First, the solution method is consistent with the physics of the flow since it uses MOC for the wave part and central differencing for the diffusion part. Second, the use of MOC allows modelers to take advantage of the wealth of strategies, methods, and analysis developed in conjunction with 1D MOC water hammer models. For example, schemes for handling complex boundary elements and strategies developed for dealing with the 1D MOC discretization problem (e.g., wave speed adjustment and interpolation techniques) can be adapted to quasi-two-dimensional MOC models. Third, although the radial mass flux is often small, its inclusion in the continuity equation by Vardy and Hwang [25] is more physically correct and accurate. A major drawback of the numerical model of Vardy and Hwang [25], however, is that it is computationally demanding. In fact, the CPU time required by the scheme is of the order N_r^3 where $N_r =$ number of computational reaches in the radial direction. Vardy and Hwang's scheme was modified by Zhao and Ghidaoui [105] to a much more efficient form. The CPU time required is reduced to order N_r, making the scheme more amenable to application to the quasi-two-dimensional modeling of pipe networks and for coupling with sophisticated turbulence models. Several numerical schemes for quasi-two-dimensional modeling are summarized in the following material.

10.1 Vardy-Hwang Scheme. The characteristic form of Eqs. (45) and (46) is as follows [25]:

$$\frac{dH}{dt} \pm \frac{a}{g}\frac{du}{dt} = -\frac{a^2}{g}\frac{1}{r}\frac{\partial q}{\partial r} \pm \frac{a}{g}\frac{1}{r\rho}\frac{\partial(r\tau)}{\partial r}$$

$$\text{along} \quad \frac{dx}{dt} = \pm a \tag{60}$$

where $q = rv$.

The pipe is divided into N_r cylinders of varying thickness. At a given time t and location x along the pipe, two equations apply to each cylinder. Since there are N_r cylinders in total, the total number of equations is $2N_r$. Therefore, the governing equations for all cylinders can be written in matrix form as follows: **Az** $=$ **b**, where **A** is a $2Nr \times 2Nr$ matrix whose form is as follows:

$$\begin{vmatrix} 1 & \frac{a}{g}+\epsilon C_{u2}(1) & & \theta C_{q2}(1)-\epsilon C_{u3}(1) & & & \\ 1 & -\left[\frac{a}{g}+\epsilon C_{u2}(1)\right] & \theta C_{q2}(1) & \epsilon C_{u3}(1) & & & \\ & \vdots & & \vdots & & \vdots & \\ 1 & \cdots & -\epsilon C_{u1}(j) & -\theta C_{q1}(j) & \frac{a}{g}+\epsilon C_{u2}(j) & \theta C_{q2}(j) & -\epsilon C_{u3}(j)\cdots \\ 1 & \cdots & \epsilon C_{u1}(j) & -\theta C_{q1}(j) & -\left[\frac{a}{g}+\epsilon C_{u2}(j)\right] & \theta C_{q2}(j) & \epsilon C_{u3}(j)\cdots \\ & \vdots & & \vdots & & \vdots & \\ 1 & \cdots & & & -\epsilon C_{u1}(Nr) & -\theta C_{q1}(Nr) & \frac{a}{g}+\epsilon C_{u2}(Nr) \\ 1 & \cdots & & & \epsilon C_{u1}(Nr) & -\theta C_{q1}(Nr) & -\left[\frac{a}{g}+\epsilon C_{u2}(Nr)\right] \end{vmatrix}$$

where $j =$ index along radial direction; $C_{u1}, C_{u2}, C_{u3} =$ coefficients associated with axial velocity u; $C_{q1}, C_{q2} =$ coefficients associated with radial flux q; and ϵ and θ are weighting coefficients. The unknown vector **z** $= H_i^{n+1}, u_{i,1}^{n+1}, q_{i,1}^{n+1}, \cdots, u_{i,j}^{n+1}, q_{i,j}^{n+1}, \cdots, u_{i,Nr-1}^{n+1}, q_{i,Nr-1}^{n+1}, u_{i,Nr}^{n+1}\}^T$ in which $i =$ index along axial direction and the superscript T de-

notes the transpose operator and $\mathbf{b}=$ a known vector that depends on head and velocity at time level n. Therefore, the solution for head, and longitudinal and radial velocities, involves the inversion of a $2N_r \times 2N_r$ matrix. The sparse nature of $\mathbf{A}$ is the reason the scheme is inefficient.

Improving the efficiency of the Vardy-Hwang scheme is essential if quasi-two-dimensional models are to become widely accepted as tools for analyzing practical pipe systems or for conducting numerical experiments. Algebraic manipulation of the coefficient matrix leads to a highly efficient scheme in which the original system becomes two subsystems with tridiagonal coefficient matrices expressed as the following: $\mathbf{Bu}=\mathbf{b}_u$ and $\mathbf{Cv}=\mathbf{b}_v$, where $\mathbf{B}$ is a tridiagonal $N_r \times N_r$ matrix given by

$$\begin{pmatrix} \dfrac{a}{g}+\epsilon C_{u2}(1) & -\epsilon C_{u3}(1) & & & \\ & & \vdots & & \\ \cdots & -\epsilon C_{u1}(j) & \dfrac{a}{g}+\epsilon C_{u2}(j) & -\epsilon C_{u3}(j) & \cdots \\ & & \vdots & & \\ & & -\epsilon C_{u1}(Nr) & \dfrac{a}{g}+\epsilon C_{u2}(Nr) \end{pmatrix}$$

The unknown vector $\mathbf{u}=\{u_{i,1}^{n+1},\cdots,u_{i,j}^{n+1},\cdots,u_{i,Nr}^{n+1}\}^T$ represents longitudinal flow velocity; $\mathbf{b}_u$ is a known vector whose elements depend on H, u, and q at time level n; and $\mathbf{C}$ is a tridiagonal $N_r \times N_r$ matrix given by

$$\begin{pmatrix} 1 & \theta C_{q2}(1) & & & \\ 0 & -[\theta C_{q1}(2)+\theta C_{q2}(1)] & \theta C_{q2}(2) & & \\ & \vdots & & & \\ \cdots & \theta C_{q1}(j-1) & -[\theta C_{q1}(j)+\theta C_{q2}(j-1)] & \theta C_{q2}(j)\cdots & \\ & & \vdots & & \\ & \cdots & \theta C_{q1}(Nr-1) & -[\theta C_{q1}(Nr)+\theta C_{q1}(Nr-1)] \end{pmatrix}$$

Lastly, $\mathbf{v}=\{H_i^{n+1},q_{i,1}^{n+1},\cdots q_{i,Nr-1}^{n+1}\}^T$ is an unknown vector of head and radial velocities and $\mathbf{b}_v=$ a known vector whose elements depend on H,u,q at time level n. Inversion of tridiagonal systems can be performed efficiently by using the Thomas algorithm.

10.2 Pezzinga Scheme. The numerical solution by Pezzinga [38] solves for pressure head using explicit FD from the continuity Eq. (47). Once the pressure head has been obtained, the momentum Eq. (48) is solved by implicit FD for velocity profiles. This velocity distribution is then integrated across the pipe section to calculate the total discharge. The scheme is fast due to decoupling of the continuity and momentum equations and the adoption of the tridiagonal coefficient matrix for the momentum equation. It has been applied to network simulations.

While the scheme is efficient, the authors have found that there is a difficulty in the numerical integration step. Since the integration can only be approximated, some error is introduced in this step that leads to spurious oscillations in the solution for pressure. To get rid of these oscillations, a large number of reaches in the radial direction may be required or an iterative procedure may need to be used [37].

10.3 Other Schemes. In Ohmi et al. [99], the averaged 1D equations are solved to produce pressure and mean velocity. The pressure gradient is then used to calculate a velocity profile using the quasi-two-dimensional momentum equation, from which wall shear stress is determined.

A similar procedure is used in Eichinger and Lein [45]. One-dimensional equations are first solved to obtain the pressure gradient. This pressure gradient is used to solve Eq. (46) using a finite difference method. The eddy viscosity is obtained from a $k-\epsilon$ model. Once the velocity profile is known, the friction term can be calculated from the velocity gradient at the wall, which is then used in the 1D equations. An iterative procedure is employed in this calculation to obtain eddy viscosity. Although there might be some difference between the discharge calculated from 1D

equations and that obtained from the velocity profile integration, it is neglected, since the calculation of the velocity profile is only used to estimate the friction term. This latter difference has only a minor influence on the calculation of the unsteady friction term, as argued by Eichinger and Lein [45].

Silva-Araya and Chaudhry's [37,98] procedure is similar to the foregoing methods. Once the velocity is obtained, energy dissipation and discharge can be calculated. The dissipation is used to estimate an energy dissipation ratio, which provides a correction factor for the friction term in the 1D equations. The adjusted 1D equations are then solved to give a new discharge, which is compared to that calculated from velocity profile integration. If the difference is small (say, less than 5%), the calculation proceeds to the next time step. Otherwise, the pressure gradient is adjusted, and the procedure is repeated. A mixing length algebraic turbulence model (smooth pipe, [37], rough pipe [98]) is used in the calculation of the velocity profile.

11 Boundary Conditions

The notion of boundary conditions as applied to the analysis of fluid transient problems is analogous to, but slightly different from, the conventional use of the terminology in solving differential equations. Just as a "boundary value" problem in the mathematical sense implies conditions that must be satisfied at the edges of the physical domain of the problem, boundary conditions in fluid transients implies the need for additional head-discharge relations to describe physical system components such as pumps, reservoirs and valves. Thus, one or more simplified auxiliary relations can be specified to solve for piezometric head, flow velocity, or other variables associated with the physical devices themselves. Examples of boundary conditions include, but are not limited to, valves, nozzles, pumps, turbines, surge tanks, air valves, tanks and reservoirs, heat exchangers, condensers and many other application-specific devices.

This section of the paper discusses a generalized approach to incorporating boundary conditions within the method of charac-

teristics framework that preserves the complex physical and topological character of the compressible fluid system. The approach utilizes unambiguous definitions of the nodes, links, and boundary conditions that represent the components of a physical pipe system or network. Attention is restricted to the method of characteristics solution because it is the most powerful and physically consistent method for dealing with physically and behaviorally complex devices without imposing unrealistic or difficult modifications to the numerical scheme. The discussion begins by reviewing the governing equations and the form of the method of characteristics solution that has been developed for this purpose.

11.1 Governing Equations and Their Solution. Two equations—a relation of mass conservation and a momentum equation—are generally used to model transient flow in closed conduits (e.g., [20–23]), which can be written from Eqs. (20), (21), and (28) as

$$\frac{\partial V}{\partial t} + \mathbf{g}\frac{\partial H}{\partial x} + \frac{fV|V|}{2D} = 0 \tag{61}$$

$$\frac{\partial H}{\partial t} + \frac{a^2}{\mathbf{g}}\frac{\partial V}{\partial x} = 0 \tag{62}$$

To be compatible, x and V must be positive in the same direction. Equations (61) and (62) are valid as long as the flow is 1D, the conduit properties (diameter, wave speed, temperature, etc) are constant, the "convective" and slope terms are small, and the friction force can be approximated by the Darcy-Weisbach formula for steady flow. In addition, it is usually assumed that the friction factor f is either constant or weakly dependent on the Reynolds number. Note that, for simplicity, the shear model in the momentum Eq. (61) above is equivalent to Eq. (41) without the convolution term. Other shear models can be readily adapted for use in the boundary condition framework described herein.

Because the equations governing transient fluid flow can seldom be solved analytically, numerical solutions are used to approximate the solution. The most widely used procedure is the fixed grid method of characteristics, which has the desirable attributes of accuracy, simplicity and numerical efficiency. The method is described in many standard references including Chaudhry [20] and Wylie et al. [23]. Again, the procedures described here can be easily adapted for use with any of the interpolation, reach-back, reach-out, and wave speed or pipe length adjustment schemes mentioned previously.

In essence, the method of characteristics combines the momentum and continuity equations to form a compatibility expression in terms of discharge Q and head H, that is

$$dH \pm BdQ \pm \frac{R}{\Delta x}Q|Q|dx = 0 \tag{63}$$

where $B = a/\mathbf{g}A$ and

$$R = \frac{f\Delta x}{2\mathbf{g}DA^2} \tag{64}$$

This equation is valid only along the so-called C^+ and C^- characteristic curves defined by

$$\frac{dx}{dt} = \pm a \tag{65}$$

For this reason, the x-t grid in Fig. 6 is chosen to ensure $\Delta x = \pm a\Delta t$. Then, if the dependent variables are known at A and B, Eq. (63) can be integrated along both AP and BP. Integration of the first two terms is straightforward, while the third requires the variation of Q with x to be known. Although this function is generally unknown, the term can usually be approximated [23]. A convenient linearization of the A to P integration is given by Karney and McInnis [106] as follows:
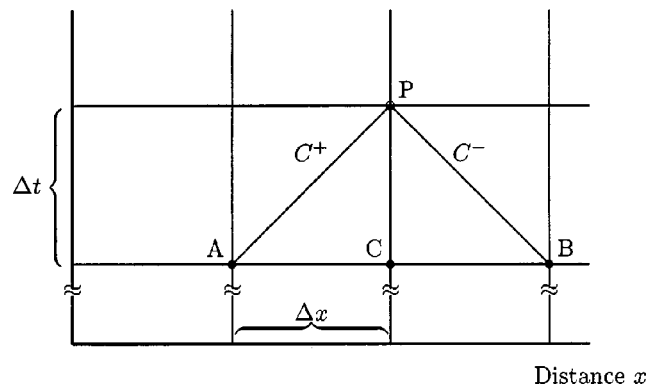

Fig. 6 Method of characteristics grid

$$\int_A^P Q|Q|dx = [Q_A + \epsilon(Q_P - Q_A)]|Q_A|\Delta x \tag{66}$$

in which $|\epsilon| \leq 1$.

This linearization of the friction term includes the "classical" $Q_A|Q_A|\Delta x$ approximation ($\epsilon = 0.0$) and the "modified" $Q_P|Q_A|\Delta x$ linearization ($\epsilon = 1.0$) as special cases. The approximation associated with $\epsilon = 0.0$ has been traditionally employed, but is troublesome for high friction cases; the modified linearization is often more accurate and has improved stability properties [107], but has not yet been universally adopted. Not only does Eq. (66) allow a single program to be used for both approximations, but intermediate values of ϵ can be used to optimize accuracy for a given Δt. Preliminary results indicate values near 0.81 are well suited to most applications. Higher-order approximations of the energy loss term can also be incorporated, but generally require iterative solution procedures. The linearized first-order approaches result in explicit formulations and provide acceptable results over the initial wave cycle for systems of low to moderate friction.

If Eq. (63) is integrated as illustrated above, two equations can be written for the unknowns at P

$$H_P = C_P - B_P Q_P \tag{67}$$

and

$$H_P = C_M + B_M Q_P \tag{68}$$

in which

$$C_P = H_A + Q_A[B - R|Q_A|(1-\epsilon)] \tag{69}$$

$$B_P = B + \epsilon R|Q_A| \tag{70}$$

$$C_M = H_B - Q_B[B - R|Q_B|(1-\epsilon)] \tag{71}$$

$$B_M = B + \epsilon R|Q_B| \tag{72}$$

In more complex systems, a subscript to indicate the pipe number is often added to these equations. At points P internal to a pipeline, H_P can be eliminated from Eqs. (67) and (68) to obtain

$$Q_P = \frac{C_P - C_M}{B_P + B_M} \tag{73}$$

At the ends of a conduit, however, the solution of the characteristic equations is algebraically complicated by one or more "boundary conditions."

11.2 Boundary Conditions. The subject of what constitutes a boundary condition can be treated generally. Karney [108] presents concise terminology for describing pipe networks and boundary conditions. His nomenclature is followed throughout this paper and is briefly reviewed here. Once the time domain is
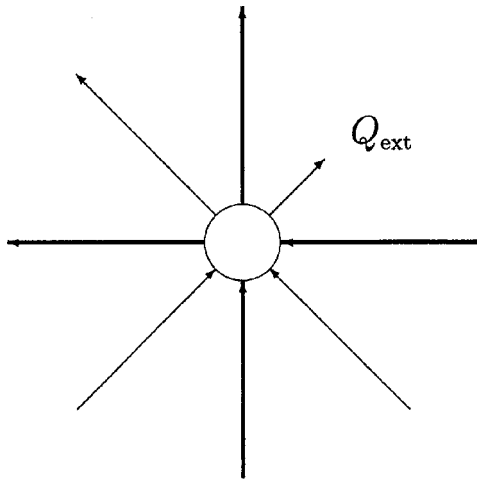
Fig. 7 Generalized node with one external flow

discretized into Δt segments, most conduits in the network are divided into one or more *reaches* of length Δx. For clarity, the term "pipe" is henceforth restricted to conduits containing at least one characteristic reach. The end of each reach, where head and flow values must be determined, is called a *section*. At sections internal to a pipe, the discharge can be obtained from Eq. (73). However, at each end of the pipe, an auxiliary relation between head and discharge must be specified. Such a head-discharge relation is called a *boundary condition*.

The term "node" is used herein to indicate a location where boundary sections meet. The *degree* of a node is the number of pipes (i.e., characteristic sections) connected to it. However, in a general network, not only pipes may be connected to a node, but various other elements as well. For example, a node may represent a suction or discharge flange of a pump, the location of a valve discharging from the network, or a connection for a pressure relief valve. All such nonpipe junctions are labeled *external* and the number of such connections is called the *complexity* of the node. A node of complexity zero is called *simple*, a node of complexity one *ordinary*, and a node of complexity greater than one *complex*. In this paper, boundary conditions associated with complex nodes are referred to as *boundary systems*. Generally, the difficulty of solving a network increases as the complexity of the nodes in the network increases but, as the following section shows, is independent of the degree of any node in the network. The terminology related to nodes can be extended in a natural way to networks as well and has been used by Karney [109] to develop a general approach for analyzing complex networks.

11.2.1 Simple and Ordinary One-Node Boundary Conditions. Junctions of several pipes are usually modeled as frictionless in transient flow applications (e.g., [109,110]). Complications arising by attempting to calculate junction losses at a general node are considerable and are not discussed in this paper. Generally, energy losses at junctions are relatively small and neglecting them does not appear to significantly impair the accuracy of the method of characteristics solution for a simple pipe junction.

The assumption that local losses are negligible is equivalent to representing the hydraulic grade line elevation at the node by a single number, designated H_P.

Consider now Fig. 7, which depicts a junction of any number of pipes at a node. Let $\mathbf{N}_1$ be the set of all pipes whose assumed flow direction is toward the node in question and $\mathbf{N}_2$ be the set of pipes whose assumed flow direction is away from the node. Let one flow be identified as external and governed by an auxiliary relation. Positive flows are assumed to be *from* the junction. The following derivation is similar to that appearing in Chapter 11 of *Fluid Transients* by Wylie and Streeter [22], but uses the notation

proposed by Karney [108]. It differs from the latter only by the inclusion of the variable friction term linearization.

For all pipes belonging to the set $\mathbf{N}_1$, Eq. (67) holds while Eq. (68) applies for members of $\mathbf{N}_2$. These equations can be rearranged to obtain

$$Q_{P_i} = -\frac{H_P}{B_{P_i}} + \frac{C_{P_i}}{B_{P_i}}, \quad i \in \mathbf{N}_1 \tag{74}$$

and

$$-Q_{P_j} = -\frac{H_P}{B_{M_j}} + \frac{C_{M_j}}{B_{M_j}}, \quad j \in \mathbf{N}_2 \tag{75}$$

in which the second subscript represents the variable at the boundary section of a particular pipe in the set.

The continuity equation for the junction requires the sum of the flows entering the node to equal the sum of the flows leaving the node

$$\sum_{i \in \mathbf{N}_1} Q_{P_i} - \sum_{j \in \mathbf{N}_2} Q_{P_j} - Q_{\text{ext}} = 0 \tag{76}$$

Equations (74) and (75) can be substituted directly into Eq. (76) to produce the following expression for H_P:

$$H_P = C_C - B_C Q_{\text{ext}} \tag{77}$$

in which

$$B_C = \left(\sum_{i \in \mathbf{N}_1} \frac{1}{B_{P_i}} + \sum_{j \in \mathbf{N}_2} \frac{1}{B_{M_j}} \right)^{-1} \tag{78}$$

and

$$C_C = B_C \left(\sum_{i \in \mathbf{N}_1} \frac{C_{P_i}}{B_{P_i}} + \sum_{j \in \mathbf{N}_2} \frac{C_{M_j}}{B_{M_j}} \right) \tag{79}$$

Equation (77) represents a single relationship between junction head H_P and external flow Q_{ext} in a multipipe frictionless junction. The form of this equation is equivalent to the single C^+ compatibility Eq. (67) and shows that any one-node boundary condition located in a network can be evaluated in exactly the same manner as if the boundary condition occurred at the downstream end of a single pipe.

Once a functional relationship representing a particular hydraulic device is substituted into Eq. (77), a single equation and unknown results. If this relationship is either linear or quadratic, an explicit formula for the unknown can be obtained.

For example, the simplest boundary condition occurs when Q_{ext} is either constant or a known function of time (e.g., constant displacement pumps or fixed demands). In this case, the value of Q_{ext} can be substituted into Eq. (77) to obtain the junction head. In particular, this equation becomes $H_P = C_C$ when Q_{ext} is zero. This solution for a simple node is algebraically equivalent to Eq. (73) if the node has only two pipes.

Comprehensive treatment of various boundary conditions such as valves, pumps, turbines, accumulators, air valves and many others can be found in Wylie et al. [23], Karney [108], Chaudhry [20], McInnis [111], Karney and McInnis [82], and McInnis et al. [112]. Formulations for many system-specific devices abound in the literature.

12 Water Hammer Software

With the advent of the Windows operating system, computer languages such as Visual Basic and Visual C, geographic information systems (GIS), and the World Wide Web, many water hammer models, previously only suited to academics and expert engineering practitioners, are now accessible to even the most novice analyst.

In this section, we describe several commercially available water hammer software packages. The information presented here is intended to aid readers in locating software appropriate to their water hammer analysis needs.

It is important to note that two of the authors of this paper are also authors of a commercially available water hammer software package. To avoid any conflicts of interest and to be fair to all water hammer software developers, a critique of each water hammer software package is not presented here.

Instead, the intention of this section is to summarize the pertinent features of each computer model. These features include, but are not limited to, the available hydraulic devices, selectable surge protection measures, input facilities, and output graphical visualization options. Also listed for each software package is the numerical method used by the water hammer model to solve the unsteady flow problem. The reader is directed to Sec. 5 for background on these numerical methods.

Each computer model has special features that distinguish it from the other reviewed models. These differences are most often the result of a desire to serve a specific commercial market. For example, some packages are best suited to fire protection sprinkler systems, fueling systems, or oil pipelines, while others are clearly tailored to large municipal water distribution systems. Still other models specialize in the analysis of hydroelectric systems, sewage force mains, or industrial applications such as cooling water systems. However, despite their obvious market focus, it is often possible to analyze just about any piping system with each of these models.

The software packages described herein are in no particular order and more information on a product (e.g., up-to-date pricing, new features, computer system requirements, etc) can be obtained upon browsing the appropriate Internet homepage, which is listed at the end of each review. Unless otherwise noted, the software packages reviewed below operate within a Windows-based environment. Please also note that the information summarized below is largely derived from each water hammer modeler's Internet homepage and is current at the writing of this paper (2003).

Due to space limitations, all of the water hammer software packages now readily available could not be included in this summary. The reader is encouraged to search out alternatives on the Internet prior to selecting one of the models described herein.

12.1 Pipenet. This fluid flow program predicts pressure surges, calculates hydraulic transient forces, models control systems, and has been commercially available for over 20 years.

The interface drag-and-drop facilities are used to build a schematic of the pipeline or network and the associated boundary devices. Pipe schedules as well as fitting, lining, pump and valve data are provided on-line for the user's convenience. The user can specify the units of both the input and output data. Fluid properties such as viscosity and specific gravity can also be input by the user. Boundary devices include pumps, air chambers, reservoirs, tanks, caissons, vacuum relief valves, check valves, flow control valves, surge relief valves, and air release valves.

PIPENET performs a surge analysis using the method of characteristics and calculates pressures and flow rates at nodes, pipes, and boundary devices, as well as transient pressure forces on pipes and bends. As an option, the program calculates the formation, growth, and collapse of a vapor cavity if the pressure in the pipe system drops to vapor pressure. PIPENET also has facilities for incorporating control theory (e.g., proportional, integral, derivative loops) in the operation of pumps and valves. Note that a special module is available for analyzing sprinkler systems.

Output data can be plotted as time history plots, each with user defined titles. Examples include pressure and flow rate time history plots at nodes, pipe sections, or boundary devices. In addition, graphs of fluid level in an air chamber versus simulation time may be plotted (Contact: www.sunrise-sys.com).

12.2 HAMMER. With HAMMER, a schematic of the piping layout for both pipelines and networks can be drawn on-screen and groups of hydraulic elements duplicated to save time during the input process. As an initial condition, steady-state data can be imported from EPANET and WATERCAD. Some of the available boundary devices include pumps, air vessels, open surge tanks, reservoirs, surge control valves, vacuum relief and air release valves, and bypass lines with check valves.

Commercially available for over 15 years, this method of characteristics-based model can be used to simulate pump power failure, valve closure, pipe breaks, and pump startup. Time history animations and plots of transient pressure, flow rate, and air or vapor volume at nodes and along pipes are available for both pipelines and networks. The model also produces profile views of network pipeline paths, showing the initial steady-state pressure as well as the maximum and minimum pressure envelopes (Contact: www.ehg.dns2go.com).

12.3 HYTRAN. Drag-and-drop facilities enable on-screen construction or deletion of a pipeline or network in either plan or profile views. Alternatively, node, pipe, and boundary device data can be directly imported from EPANET. Some of the selectable boundary devices include pumps, turbines, air chambers, vacuum relief valves, check valves, tanks, reservoirs, pressure relief valves, pressure regulating valves, and demands. On-line help, including a database of valve coefficients and pipe material properties, is available to the user.

A method of characteristics-based solver generates pressure and flow rate history traces at nodes and along the pipeline following pump power failure or startup. In addition, the computed transient hydraulic grade line at any instant in simulation time can be plotted in combination with the pipeline profile. Pressure traces, hydraulic grade line plots, and pipe flow direction can be animated for real-time viewing. A column separation indicator warns the user when cavitation is detected (contact: www.hytran.net).

12.4 HYPRESS. This model has an object-oriented interface that allows for flexible input of pipe, node, and boundary device data for pipelines and networks. Some of the boundary devices that can be represented by the model include pumps, turbines, valves, reservoirs, surge chambers, and air vessels.

Using a fourth-order implicit finite difference based numerical solver, HYPRESS calculates the maximum, minimum, and instantaneous transient hydraulic grade line for a pipeline following pump power failure. The hydraulic grade lines are plotted in combination with the pipeline elevation profile and the instantaneous transient hydraulic grade line, which can be animated in real time (Contact: www.hif.cz).

12.5 IMPULSE. Liquids such as water, petroleum, chemical products, cryogens, and refrigerants can all be modeled using the IMPULSE water hammer model. A piping schematic is created in the workspace using drag-and-drop facilities and data can be input directly by the user or obtained from a built-in database containing properties for nine fluids and eight pipe materials. Some of the hydraulic devices that can be incorporated into the pipe network include pumps, reservoirs, liquid accumulators, gas accumulators, vacuum breaker valves, demands, relief valves, and pressure control valves.

IMPULSE will calculate a system steady state and transfer it to the method of characteristics solver. Pipe length adjustment, as opposed to wave speed adjustment, is used in combination with the time step to spatially discretize the piping network. In some cases, this means that the modeled pipe length can approximate the true length of the pipe. Transient events (e.g., pump power failures, pump starts, valve closures, etc) can be initiated based on time or a device setpoint. Liquid column separation, vapor cavitation, and cavity collapse can be modeled. This model will identify when and where maximum pressures occur and plot flow rate, pressure, and velocity time histories, which can be formatted by

the user. At each time interval, output, such as maximum and minimum pressures, are tabulated for each node, pipe, and boundary device (Contact: www.aft.com).

12.6 WANDA. Both pressurized and nonpressurized branched and looped pipe systems can be simulated with this water hammer model. Free-surface flow (i.e., a partly filled pipe) is modeled using a conjugate gradient method with an upwind advection approximation. The effects of draining and filling a pipeline can be simulated with this component.

A schematic of the piping system can be created on-screen using a palette of boundary devices. A user defined image (e.g., a street map) can be imported as a background to the schematic and properties of nodes, pipes, and boundary devices are input using dialog boxes. Some of the available boundary devices include pumps, control valves, check valves, taps, air vessels, air inlet valves, surge towers, pressure relief valves, weirs, and condensers.

The method of characteristics-based solver can be interrupted and resumed during a simulation. Cavitation and control theory (e.g., proportional integral derivative loops, sensors, etc) modules are optional. Pressure versus time histories can be plotted at user-defined locations within the pipe system. In addition, it is possible to view an animation of pressure wave propagation and reflection along pipeline routes of a network (Contact: www.wldelft.nl/soft/wanda/).

12.7 FLOWMASTER. This model calculates transient pressures and flow rates in piping networks. In addition, calculation of heat transfer and simulation of partly empty pipe segments (e.g., sprinkler systems) is possible.

Pipe networks can be drawn on-screen using a list of piping components and some of the boundary devices that can be represented include pumps, reservoirs, weirs, orifices, valves, accumulators, diaphragms, diffusers, heat-exchangers and pipe fittings. User-defined boundary devices can be programmed in either FORTRAN or C. Operational issues can be studied using predefined controllers or user-defined controllers programmed in Visual Basic or Java.

The method of characteristics solver generates results that can be viewed graphically or in tabular formats. Note that in addition to liquids, gas flow dynamics can be simulated (Contact: www-.flowmaster.com).

12.8 SURGE2000. With this model, a schematic of the piping layout can be drawn on-screen and over it can be placed an imported background image, such as a street or elevation contour map. Boundary devices include pumps, valves, reservoirs, tanks, air vessels, air and vacuum valves, pressure relief valves, surge anticipating valves, and heat exchangers.

This model uses the wave-plan method as opposed to the method of characteristics or finite difference methods employed by the other models reviewed in this paper. Pump power failure, pump startup, and valve operations (e.g., closure) are just some of the unsteady fluid flow events that can be simulated with SURGE2000. Output, such as pressures, can be tabulated, plotted as contours over the system map, and displayed in time history plots at nodes. In addition, for each pipeline path, the maximum, minimum, and instantaneous transient hydraulic grade lines can be plotted on an elevation versus distance graphic (Contact: www.kypipe. com).

12.9 LIQT. First introduced in 1972, LIQT can model fluid transients in pipelines and networks subject to pump power failure and startup, turbine load loss, and valve closure. Some of the boundary devices that can be selected by the user include pumps, turbines, check valves, air and vacuum valves, surge tanks, standpipes, accumulators, and pressure relief valves. LIQT operates within a DOS environment window and uses the method of characteristics to compute pressures and flow rates that can be exported to spreadsheets, databases, and graphic software for presentation (Contact: www.advanticastoner.com).

12.10 WHAMO. This model uses a four-point implicit finite difference method to calculate time-varying flow and head in pipelines and networks. The user can select boundary devices such as pumps, turbines, valves, tanks, reservoirs, vented or unvented air chambers, pressure control valves, electric governors, and constant or time varying demands. A schematic of the piping system can be drawn on-screen with the help of a palette of boundary device symbols.

Both steady-state and transient conditions are generated and simulations of pump power failure, valve closure, turbine load rejection, turbine startup, and governor controlled turbine operation are possible (Contact: www.cecer.army.mil/usmt/whamo/whamo.htm).

12.11 TRANSAM. Using this model, real-time, 3D (i.e., distance, time, and pressure) animations of the transient pressure surface can be viewed along user-defined network and pipeline paths. A piping layout map can be created in a designated workspace using point-and-click options and a combination of pull-down menus and dialog boxes are available for node, pipe, and boundary device data input. An EPANET to TRANSAM conversion utility is supplied. Some of the boundary devices that can be represented by this model include pumps, turbines, air chambers, reservoirs, tanks, flow control valves, air and vacuum relief valves, check valves, pressure relief valves, surge anticipating valves, pressure reducing/sustaining valves, constant and time varying demands, and bypass lines with check valves.

Pump power failure and startup, variable speed pump and valve operations (e.g., full and partial openings or closures), turbine load rejection, and pipe breaks are just some of the event or time initiated unsteady flow conditions that can be simulated using this method of characteristics-based model. Simulation of the formation, growth, and collapse of vapor cavities is optional. Time history plots of pressure (and flow rate at nodes) can be produced at nodes and along pipes. Real-time animations of the instantaneous transient, maximum, and minimum hydraulic grade lines can be viewed for pipe paths (Contact: www.hydratek.com).

13 Emerging Applications in Water Hammer

By now, the reader is likely aware that the principal use of transient analysis, both historically and present day, is the prediction of peak positive and negative pressures in pipe systems to aid in the selection of appropriate strength pipe materials and appurtenances and to design effective transient pressure control systems.

Two important areas in which transient modeling is now taking a key role are parameter estimation for leakage detection and water quality predictions in potable water systems. Brief discussions of these two important areas of application are provided in this section.

13.1 Parameter Estimation for Leakage Detection and Inverse Models. In many pipeline related industries, such as a potable water supply or in oil or gas transmission, owners know that information is the key to successful management of their pipeline operation. For example, in the case of a water supply, physical system characteristics, customer data, production rates, maintenance records, quality assays, and so on, each provide management, engineering, operations, and maintenance staff with information they need to keep the system running efficiently and safely, and at a reasonable cost to the consumer. A large body of literature on the subject of information requirements and data management already exists, and all private and public pipeline utilities are aware of the importance of collecting, archiving, and analyzing data. Perhaps the most costly and time consuming aspect of information management, however, is the collection of data. This section outlines how inverse transient analysis can be applied to gather some types of physical system data. The technology has the potential to be both cost efficient and accurate.

Using high-frequency pressure transducers, it is now possible to safely measure induced, or naturally occurring, pressure surge events. Coupling water hammer models to inverse models offers the possibility of inexpensive data collection with a wide coverage of the system. System demands, leakage, pipe condition (roughness), closed or partially closed valves, even pockets of trapped gas or air can (in theory at least) all be detected using recorded high-frequency pressure data. In addition to pressure measurements, transient flow data can also be used in the inverse analysis procedures. However, flow meters capable of accurately resolving the variation in flow rates that occurs during water hammer events are quite expensive and more troublesome to install. High-frequency pressure transducers, on the other hand, are relatively inexpensive and easy to mount at common access points, such as valve and meter chambers, or even at fire hydrants. To date, hydraulic model parameters such as pipe roughness and wave speeds have been successfully calibrated using these techniques.

13.1.1 Inverse Analysis of Transient Data. Whether a transient is small or large, accidental or planned, pressure waves propagate from their respective points of origin to other parts of the system. They travel at speeds ranging from about 250 m/s to nearly 1500 m/s, depending on pipe material, soil and anchoring conditions. The shock fronts interact with any part of the system that either dissipates energy or does work in a thermodynamic sense. Thus, the energy content of the wave is diminished by virtue of its interaction with the physical system, and its frequency components, amplitude, phasing, and attenuation characteristics become modified through successive interaction with the system. In effect, a pressure signal at a given location constitutes a record of conditions in the system during the course of a given transient event.

Deciphering this record of interaction and extracting its information content is precisely what an inverse transient model does. The inverse model evaluates the recorded pressure (or flow) signal and determines which set (or sets) of system parameters, i.e., pipe roughness, water consumption (leakage), wave speed, etc, best matches the measured data. In this way, information (data) of several types can be gathered from those areas of the pipe system that the transient waves have traversed. For example, pressure traces from two pump trip tests can be sufficient to estimate pipe roughness values for every major pipe and consumption values at each node in a small city. Of course, the accuracy of the estimates can be improved by increasing the number of tests performed or by monitoring pressures (flows) at more than one location.

There is extensive literature about inverse analysis in both scientific and engineering journals. The techniques have been applied for many years to structural engineering applications e.g., system identification and damage detection [113]. Sykes [114], Sun and Yeh [115], and Sun [116] have used inverse methods to identify parameters in 2D groundwater flow. Jarny et al. [117] applied the adjoint technique to heat conduction problems. Cacuci et al. [118] and Hall [119] applied the adjoint method to meteorology and climate modeling. Marchuk [120] applied the adjoint technique to air pollution problems.

Most, though not all, inverse models utilize real measurements in a "data-fitting" exercise that typically provides "best-fit" parameters for the mathematical model postulated to fit the data. Least-squares data-fitting is a simple example of an inverse method that tries to fit the best mathematical model (i.e., linear, exponential, polynomial, etc) to some observed data set. The "goodness of fit," i.e., how well the particular assumed mathematical model represents the data, can be measured statistically by an analysis of the errors between the observed data and those predicted by the model. In fact, these errors are explicitly minimized using Lagrangian optimization such that the optimal parameter set is directly solved for.

The same concept can be applied to more complex physical systems using sophisticated models. In an inverse problem, output from a "forward" model is used to generate an estimate of one or more measured data sets using some assumed set of system parameters. System parameters could be pipe wave speed, friction factor, water consumption rates and locations, leakage rates and locations, and so on. A "merit" function is used to compare the goodness of fit between the observed data and the model output. Common merit functions are the error sum of squares, sum of the absolute values of errors, etc. Some sort of search or optimization procedure is employed to find the set of parameter values that minimizes the discrepancy between observed data values and those predicted by the forward model. It is the nature of the search technique employed in the optimization step that characterizes the inverse modeling approach.

13.1.1.1 Adjoint models. Adjoint models use a form of Lagrangian optimization coupled with a gradient search to minimize the errors between the observed data and the forward model prediction. In transient flow applications, the problem statement would take the following general form (see also Liggett and Chen [121]):

$$\text{Minimize} \quad E = \sum \left[(h^m - h^c)^2 + (q^m - q^c)^2 \right] \qquad (80)$$

subject to the following physical constraints:

$$\frac{\partial h}{\partial t} + \frac{a^2}{\mathbf{g}A} \frac{\partial q}{\partial x} = 0 \qquad (81)$$

$$\frac{\partial q}{\partial t} + \mathbf{g}A \frac{\partial h}{\partial x} + f \frac{q|q|}{2AD} = 0 \qquad (82)$$

where E is the error sum of squares and Eqs. (81) and (82) are the continuity and momentum equations rewritten in terms of discharge and assuming steady Darcy-Weisbach friction. The superscript m denotes measured data values and the superscript c denotes the values computed by the forward model, h is piezometric pressure head, q is the flow rate, a is the pipeline celerity, f is the Darcy-Weisbach friction factor, t is time, x is a spatial coordinate, $\mathbf{g}$ is gravitational acceleration, and A and D are the pipeline cross-sectional area and diameter, respectively.

Equation (80) can be combined with Eqs. (81) and (82) by using Lagrangian multipliers λ_1 and λ_2 as follows:

$$E^* = \int_x \int_t \left[(h^m - h^c)^2 \delta(x^m - x^c) \delta(t^m - t^c) + (q^m - q^c)^2 \delta(x^m - x^c) \delta(t^m - t^c) + \lambda_1 \left(\frac{\partial h}{\partial t} + \frac{a^2}{\mathbf{g}A} \frac{\partial q}{\partial x} \right) + \lambda_2 \left(\frac{\partial q}{\partial t} + \mathbf{g}A \frac{\partial h}{\partial x} \right. \right.$$
$$\left. \left. + f \frac{q|q|}{2AD} \right) \right] dx \, dt \qquad (83)$$

The merit (error) function has now been designated E^* to indicate that it includes the Lagrangian terms for the continuity and momentum equations, and has been expressed as an integral to be consistent with the continuum form of the momentum and continuity equations. The Dirac delta functions are included to ensure that merit function terms are evaluated only at those locations and times for which observed data exist, i.e.,

$$\delta(x^m - x^c) = \begin{cases} 1 & \text{for} \quad x^m = x^c \\ 0 & \text{for} \quad x^m \neq x^c \end{cases}$$

$$\text{and} \quad \delta(t^m - t^c) = \begin{cases} 1 & \text{for} \quad t^m = t^c \\ 0 & \text{for} \quad t^m \neq t^c \end{cases} \qquad (84)$$

The conventional approach to Lagrangian optimization is to take partial derivatives of the merit function with respect to the unknown system parameters (a or f in this simple formulation) and the Lagrangian multipliers λ_1 and λ_2, and equate these slope functions to zero. This provides four equations from which the four unknown variables a, f, λ_1, and λ_2 could be determined.

However, as these equations are quasi-linear hyperbolic partial differential equations, a more elaborate procedure must be used. Partial derivatives of the merit function are taken with respect to λ_1 and λ_2 and at critical points of the merit function must have a slope of zero. The two derivative functions given in Eq. (85) below are known as the adjoint equations.

$$\frac{\partial E^*}{\partial \lambda_1} = \frac{\partial h}{\partial t} + \frac{a^2}{\mathbf{g}A}\frac{\partial q}{\partial x} = 0$$

$$\text{and} \quad \frac{\partial E^*}{\partial \lambda_2} = \frac{\partial q}{\partial t} + \mathbf{g}A\frac{\partial h}{\partial x} + f\frac{q|q|}{2AD} = 0 \quad (85)$$

It suffices to say that the adjoint model is solved iteratively. Values for physical system parameters a and f are assumed, and the forward model is run to determine the transient head and flow. The adjoint equations are solved using the known heads and flows in a backward pass to calculate the Lagrangian parameters λ_1 and λ_2. These values are used in a gradient search step (the conjugate gradient technique is often used) to select new estimates of the optimal parameters. The search procedure terminates when the value of E^* cannot be reduced any further.

The advantage of the adjoint method is that it can be extremely efficient for a well-conditioned problem. The model can be formulated to solve for other parameters of interest beside wave speed and friction.

13.1.1.2 Genetic algorithms.   Genetic algorithms (GAs) have gained widespread popularity in recent years. There are many reasons for this success: (i) GAs can be applied to a wide variety of problems; (ii) GAs do not require the development of additional code needed to solve the adjoint of the forward problem; (iii) a single GA can be used with various models that solve the same forward problem; (iv) any model parameters can be specified as the unknown system parameters in a GA; (v) GAs are quite successful in problems containing local extrema; and (vi) GAs can find not only the global optimum, but can also describe other suboptimal solutions of interest, particularly for flat merit functions. Genetic algorithms do not work for every problem, however, and one must be aware of their limitations. GAs work best for problems in which genotypes consist of a small number of genes that can be expressed in short length strings, i.e., problems having few decision variables (parameters) that can be identified by a small number of binary digits. Problems with large numbers of real-valued parameters over an extensive and continuous domain are demanding of computer resources when solved by genetic algorithms. Despite these limitations, the method seems to work well with pipeline problems, albeit solution procedures are slower than those of the adjoint method.

In the simplest sense, genetic algorithms are an efficient form of enumeration. A candidate set of parameters is assumed or randomly generated to form individuals in a population. Subsequent iterations use evolutionary (mutation) and reproductive (crossover) functions to generate further generations of solutions. The mathematical principle upon which genetic algorithms are based is intended for use with problems in which the decision variables are discrete, and in these situations the method can be extremely efficient. Modifications to the method have been developed to extend its application to continuous real-valued problems, although the procedures are less efficient in these cases.

Karney and Tang [122] have successfully applied the genetic algorithm method to parameter estimation problems in water distribution systems using transient pressure readings. Using data from only two pump trip tests (one for model validation and the other for the parameter estimation), Karney and Tang have successfully estimated pipe roughness factors and wave speed for several large water distribution systems.

13.1.1.3 Pressure wave method.   Brunone [123] and Brunone and Ferrante [124] conducted numerical and physical experiments to investigate the possibility of using transient data for leakage

detection. The transient response of a pipeline system to a given flow disturbance with and without leakage points was measured as well as computed. The influence of the size and shape of small leaks, along with discharge conditions and initial flow regime, on the transient response of a pipeline system were analyzed. It is found that the influence of the leak on the shape and amplitude of the pressure signal is quite noticeable, even when the leak flow is only a few percent of the total flow in the pipe. Therefore, Brunone [123] and Brunone and Ferrante [124] formulated a scheme for leakage detection on the basis of studying the difference in transient response of a pipeline system with and without a leak. It is observed that the measured pressure head traces for the pipeline with a leak is different from that for an intact pipe. When the transient wave encounters a leak, part of the wave is reflected back. The leak location is determined from the time when the reflected wave arrives at the measurement station. The leak induces additional drop in the pressure head traces, the amount of drop depending on the size of the leak. The size of the leak is using a formal inverse approach. The agreement between the actual and the computed location and size of leak points is good.

13.1.1.4 Frequency response method.   The frequency response method is used by Mpesha et al. [125,126]. A hydraulic system is made up of several components. Each component can be represented by a transfer matrix. Transient flow is caused by the periodic opening and closing of a valve [125] or by the sudden opening or closing of a valve [126]. A frequency response diagram at the valve is developed based on the transform matrix. For a system with leaks, this diagram has additional resonant pressure amplitude peaks that are lower than the resonant pressure amplitude peaks for the system with no leaks. From the frequency of the peaks, the location of the leak can be detected. Very good agreement have been obtained between the computed and the real leak condition.

In Ferrante and Brunone [127], the governing equations for transient flow in pipes are solved directly in the frequency domain by means of the impulse response method. Therefore, the solution of the response of the system to more attractive transient events is available. Harmonic analysis of the transient pressure is used to identify the location and the size of a leak.

13.1.1.5 Mode damping method.   Wang et al. [128] investigated the damping characteristics of a transient pressure wave by wall friction and by system leakage. It is found that wall friction damps all modes similarly, but leakage damps different Fourier modes differently. In addition, mode damping by leakage is found to depend on leak location. The marked difference in mode damping between wall friction and system leakage was successfully used to identify the location and size of leaks [128]. In particular, Wang et al. [128] were able to accurately identify system leaks by investigating mode damping characteristics of transient pressure data obtained from numerical as well as laboratory studies. The damping characteristic technique was successfully applied to single and multiple leaks.

13.1.1.6 Wavelet transform method.   Frequency analysis can only deal with a stationary signal (i.e., the signal has to be either periodic or decomposable into a set of periodic signals). Wavelet transform can be used to detect local singularities in a measured signal. Whenever there is a singularity in a measured signal, a local maximum of the transform coefficient for the measured signal appears. The application of the transient wavelet transform to leakage detection in a pipeline was pioneered by Ferrante and Brunone [129]. The wavelet transform of pressure head history is performed. According to the transform of the signal, the discontinuities in pressure head traces are detected. These discontinuities correspond to wave reflections at boundary elements and at leak points. Using the time at which a discontinuity is observed, the

distance between the leak and the measurement station can be calculated. The location found by wavelet transform agrees with the real location very well.

13.1.1.7 Identifiability and uniqueness requirements. In order for any inverse method to be successfully applied, two key mathematical properties of the problem must be satisfied: identifiability and uniqueness. Identifiability refers to the notion that a single set (or a finite number of distinct sets) of parameter values must reproduce, within an established level of error, the same response exhibited by the actual system. Uniqueness means that the merit function exhibits a single, global minimum. For complex problems, there is no rigorous mathematical procedure that can assure us that identifiability and uniqueness requirements are satisfied in general. However, a simple example is described in the following section that provides insight into the suitability of different inverse modeling techniques for pipeline transient problems.

13.1.1.8 Identifiability. Let $\mathbf{H}_m = \{H_0, H_1, H_2, \ldots, H_n\}$ denote a set of measured values, e.g., piezometric head, at time steps 0 to n corresponding to some sampling rate $(t_n - t_0)/(n - 1)$. Let $\mathbf{h_c} = \{h_0, h_1, h_2, \ldots, h_n\}$ similarly denote the set of computed heads at the same time steps but for a particular pair of unknown, but desired, parameter values σ_1 and σ_2. Then, the following criterion for identifiability can be stated:

Identifiability criterion: A set of parameter values σ_1 and σ_2 are identifiable if and only if $\mathbf{H}_m \equiv \mathbf{h_c} \pm \epsilon$, where ϵ represents the absolute value of data, measurement, and model error. The identifiability criterion can be visualized by plotting the difference between $\mathbf{H}_m$ and $\mathbf{h_c}$ for each pair of feasible values of parameters σ_1 and σ_2 in the domain and selecting the zero contour of the differences. Identifiable parameter pairs for which $\mathbf{H}_m \equiv \mathbf{h_c}$ would appear as intersections (loci of intersecting lines) of all such contours.

Uniqueness: The second condition that needs to be met if adjoint methods are to be used with a reasonable expectation of success is uniqueness, i.e., there should ideally be only a single critical point of the merit function within the feasible search domain.

The adjoint technique can still be useful if the feasible search domain can be restricted to a smaller region containing the global minimum. To this end, a more robust optimization scheme is often employed to locate the probable region of the global minimum. Following this initial screening, the adjoint scheme can then be applied to refine the solution. This two-phase optimization approach is only worthwhile if the time required to find a global minimum by other methods is too costly. Compared to the adjoint technique, genetic algorithms are better suited to solving problems with multiple critical points and those that appear to give good results for inverse modeling in pipeline transient applications.

13.2 Pathogen Intrusion in Water Supply Systems. In the first sentence of its proposed Ground Water Rule: Public Health Concerns document, the U.S. EPA Office of Water states that, "Assurance that the drinking water is not contaminated by human or animal fecal waste is the key issue for any drinking water system." The proposed Ground Water Rule is designed to protect against pathogenic bacteria and viruses in source water, against growth of opportunistic pathogenic bacteria in ground water distribution systems, and to mitigate against any failure in the engineered systems, such as cross-connections or sewage infiltration into distribution systems.

There is considerable evidence in the literature that the number of disease outbreaks (including a large number that are unreported [www.epa.gov/orgwdw000/standard/phs.html]) due to fecal contamination of distribution systems is already large and might be growing. From 1971–1994, 50 of 356 reported waterborne disease outbreaks occurred as a result of pathogen entry into distribution systems. More recent statistics from the U.S. Center for Disease Control put the ratio of distribution system intrusions to other sources of drinking water contamination as high as 1:1. Studies by Payment [130] suggest that one third of the 99 million gastroenteritis cases in the U.S. each year might involve exposure to waterborne pathogens in the distribution system. Conservatively estimating that 20% of these cases result from pathogen intrusion into water pipes, then, in America alone, as many as 20 million cases of gastroenteritis annually might be directly caused by contamination of drinking water distribution systems.

Recent research into the problem is now attempting to address four critical questions that naturally arise in response to these alarming statistics. (i) What is the nature of the pathogen intrusion mechanism(s)? (ii) Why don't routine water sampling and laboratory testing detect intrusion events? (iii) Is the health of water consumers in a particular system at risk? (iv) Can the risk of distribution system intrusions be reduced (and by how much) or eliminated altogether? Answers to these four questions depend entirely on developing a clear understanding of the complex interactions with hydraulic transients in pipe systems.

13.2.1 Distribution System Intrusion Pathways. There are several potential intrusion pathways whereby bacterial, protozoan, and viral pathogens can enter a water supply, transmission, or distribution pipeline: (i) at the source; (ii) during loss of pressure and subsequent exposure of the pipe interior to the external air, soil or groundwater (such as may happen during a main break repair); (iii) via cross-connections on a consumer's property; and (iv) via cross-connections in the distribution system.

The first two intrusion mechanisms are "controlled" situations insofar as the quality of finished water is carefully monitored and treated to ensure compliance with drinking water standards, while the latter two pathways are largely "uncontrolled." Cross-connections can arise whenever a possible source of contaminated water or other liquid can be introduced into the potable water system by virtue of backpressure (an excess of pressure causing flow to occur in a direction opposite to its normal intended flow direction) or siphonage (suction or "negative" pressure inducing flow from a contamination source into the distribution system). While backpressure and negative pressures are usually eliminated through proper hydraulic design, there is one major source of negative pressures that is not normally accounted for in distribution system design—hydraulic transients.

Water hammer occurs regularly in some systems and periodically in others whenever flow conditions are changed rapidly. Whether these changes in flow are the result of planned operations like pump starts and stops, or are unplanned events initiated by power outages, accidental valve closures, or rupturing of a pipe, the ensuing episodes of negative pressure can introduce contaminated fluids into the pipeline. Contamination can occur on a customer's property or on the utility side of a service connection. Contaminated fluids introduced at a cross-connection would be largely transported in the prevailing direction of flow in the pipe after entering the system.

Pressure dependent leakage is commonly known to occur from the potable system to the surrounding (soil) environment through pipe joints, cracks, pinholes, and larger orifice-like openings. Funk et al. [131] developed analytic hydraulic parameters to assess the potential for transient intrusion in a water distribution system. Their intrusion model was based on the percentage of water lost through leakage lumped at system nodes and an "equivalent orifice" needed to pass the discrete leakage flow at the prevailing system pressure.

A paper by McInnis (in progress) extends the work of Funk et al. to incorporate alternative intrusion flow models based on laminar flow, turbulent orifice flow, or a mixture of the two flow types. Work done by Germanopoulos and Jowitt [132] on pressure dependent leakage suggests that most distributed leakage is probably laminar in nature, occurring through larger numbers of small openings. The 2D water hammer equations with turbulence models developed by Vardy and Hwang [25], Pezzinga [38], and Silva-Araya and Chaudhry [37,98] will be useful in generating

models for predicting intrusion volumes, initial distribution of contaminant concentrations in the pipes, and the ultimate fate of contaminants within the distribution system.

McInnis [133] expands the consideration of transient intrusion events from purely fluid mechanics aspects by developing a risk-based framework for comparing the actual human health risks and relative risk reduction achieved by alternative transient-intrusion mitigation strategies. McInnis [133] applies transient modeling with some assumed reference groundwater contamination level and computes hypothetical intrusion volumes for a given transient event to predict the transitory impact of the event on system water quality. He has also proposed meaningful risk-based measures to provide quantitative comparisons of the relative reduction in the risk of receptor infection achieved by alternative mitigation strategies.

14 Practical and Research Needs in Water Hammer

Both theory and experiments confirm the existence of helical type vortices in transient pipe flows. The conditions under which helical vortices emerge in transient flows and the influence of these vortices on the velocity, pressure, and shear stress fields are currently not well understood and, thus, are not incorporated in transient flow models. Future research is required to accomplish the following:

1) understand the physical mechanisms responsible for the emergence of helical type vortices in transient pipe flows
2) determine the range in the parameter space, defined by Reynolds number and dimensionless transient time scale over which helical vortices develop
3) investigate flow structure together with pressure, velocity, and shear stress fields at subcritical, critical, and supercritical values of Reynolds number and dimensionless time scale

The accomplishment of the stated objectives would be sought through the use of linear and nonlinear analysis. Understanding the causes, emergent conditions, and behavior of helical vortices in transient pipe flows as well as their influence on the velocity, pressure, and shear stress field are fundamental problems in fluid mechanics and hydraulics. Understanding these phenomena would constitute an essential step toward incorporating this new phenomena in practical unsteady flow models and reducing significant discrepancies in the observed and predicted behavior of energy dissipation beyond the first wave cycle.

Current physically based 1D and 2D water hammer models assume that (i) turbulence in a pipe is either quasi-steady, frozen or quasi-laminar; and (ii) the turbulent relations that have been derived and tested in steady flows remain valid in unsteady pipe flows. These assumptions have not received much attention in the water hammer literature. Understanding the limitations and accuracy of assumptions (i) and (ii) is essential for establishing the domain of applicability of models that utilize these assumptions and for seeking appropriate models to be used in problems where existing models fail. Preliminary studies by Ghidaoui et al. [46] show that agreement between physically based 1D and 2D water hammer models and experiments is highly dependent on the Reynolds number and on the ratio of the wave to turbulent diffusion time scales. However, the lack of in-depth understanding of the changes in turbulence during transient flow conditions is a significant obstacle to achieving conclusive results regarding the limitation of existing models and the derivation of more appropriate models. Therefore, a research program whose main objective is to develop an understanding of the turbulence behavior and energy dissipation in unsteady pipe flows is needed. This research program needs to accomplish the following:

1) improve understanding of and the ability to quantify changes in turbulent strength and structure in transient events at different Reynolds numbers and time scales
2) use the understanding gained in item 1 to determine the range

of applicability of existing models and to seek more appropriate models for problems where current models are known to fail

The development of inverse water hammer techniques is another important future research area. A number of very promising inverse water hammer techniques have been developed in the last decade. Future work in this area needs to accomplish the following:

1) further investigate the issues of efficiency, reliability, and identifiability of inverse water hammer techniques
2) develop more realistic laboratory and field programs in order to further test existing inverse techniques as well as develop new ones
3) develop systematic approaches (e.g., using stochastic methods) that can incorporate the influence of modeling and measurement errors on the reliability of inverse methods
4) develop identifiability-based methods to determine the quantity and quality of data necessary to carry out a successful inverse program

The practical significance of the research goals stated above is considerable. An improved understanding of transient flow behavior gained from such research would permit development of transient models able to accurately predict flows and pressures beyond the first wave cycle. One important consequence of this is that the behavioral aspects of control devices activated (or reactivated) by local flow or pressure is correctly modeled. Most importantly, however, reducing the modeling errors beyond the first wave cycle, along with better inverse techniques, will greatly improve the accuracy and reliability of inverse transient models. This is important because inverse models have the potential to utilize field measurements of transient events to accurately and inexpensively calibrate a wide range of hydraulic parameters, including pipe friction factors, system demands, and leakage. At this time, such information can only be obtained through costly field measurements of flows and pressures conducted on a few individually sampled pipes in the system. Transients, on the other hand, traverse the entire system, interacting with each pipe or device in the system. Thus, they contain large amounts of information regarding the physical characteristics of the system. Inverse transient analysis techniques are now being developed to decode this information for hydraulic model calibration as well as to identify and locate system leakage, closed or partially closed valves, and damaged pipes. The potential annual savings in routine data collection costs for water supply utilities world wide is significant. Equally important, an improved understanding of the true nature of turbulence in transient flows will be a groundbreaking step toward modeling transient-induced water quality problems. Negative pressure waves can cause intrusion of contaminants from the pipe surroundings through cracks, pinholes, joints, and ruptures in the pipes. In addition, water hammer events cause biofilm sloughing and resuspension of particulates within the pipe, potentially leading to unsafe or unpleasant drinking water. Without a better understanding of transient flow behavior, the risk and degree of contamination of water supply systems during transient events cannot be quantitatively assessed.

15 Summary

The scientific study of transient fluid flow has been undertaken since the middle of the nineteenth century. As is true of every other area of engineering research, a great many advances have been made in the accuracy of analysis and the range of applications since then. Although only a few simple problems were approachable by earlier analytical methods and numerical techniques, a much broader spectrum of transient problems could be solved once graphical methods were developed. More recently, the application of digital computing techniques has resulted in a rapid increase in the range and complexity of problems being

studied. This paper provides both a historical perspective and review of water hammer theory and an overview of recent developments in this field of fluid mechanics.

Specifically, advances in the last one or two decades dealing with some of the more complex and fundamental fluid mechanics issues have been discussed:

1) The relation between state equations and wave speeds in single as well as multiphase and multicomponent transient flows are illustrated and discussed.
2) Various forms of 1D and 2D water hammer equations, such as the Joukowsky model, classical 1D waterhammer equations, the 2D plane wave equations, and the quasi-two-dimensional plane wave equations are derived.
3) Governing equations of turbulent water hammer flows are obtained by ensemble averaging of the quasi-two-dimensional plane wave equations.
4) Order of magnitude analysis is used throughout the paper to evaluate the accuracy of the assumptions in the various forms of water hammer governing equations.

Water hammer models are becoming more widely used (i) for the design, analysis, and safe operation of complex pipeline systems and their protective devices; (ii) for the assessment and mitigation of transient-induced water quality problems; and (iii) for the identification of system leakage, closed or partially closed valves, and hydraulic parameters such as friction factors and wave speeds. In addition, turbulence models have been developed and used to perform numerical experiments in turbulent water hammer flows for a multitude of research purposes such as the computation of instantaneous velocity profiles and shear stress fields, the calibration and verification of 1D water hammer models, the evaluation of the parameters of 1D unsteady friction models, and the comparison of various 1D unsteady friction models. Understanding the governing equations that are in use in water hammer research and practice and their limitations is essential for interpreting the results of the numerical models that are based on these equations, for judging the reliability of the data obtained from these models, and for minimizing misuse of water hammer models.

Acknowledgments

Nomenclature

$\mathbf{A}$ - system matrix
A - cross-sectional area of pipe
a - water hammer wavespeed
a - coefficient for five-region turbulence model
$\mathbf{B}$ - matrix for subsystem of longitudinal velocity component
B - coefficient for MOC formulation
B_C - lumped quantity for characteristics solution for pipe network
B_M - quantity for negative characteristics used for 1D MOC solution
B_P - quantity for positive characteristics used for 1D MOC solution
$\mathbf{b}$ - known vector for system
$\mathbf{b}_u$ - known vector for subsystem of longitudinal velocity component
$\mathbf{b}_v$ - known vector for subsystem of head and radial component
$\mathbf{C}$ - matrix for subsystem of head and radial velocity component
C_B - coefficient for five-region turbulence model
C_C - lumped quantity for characteristics solution for pipe network
C_c - coefficient for five-region turbulence model

C_M - quantity for negative characteristics used for 1D MOC solution
C_m - coefficient for five-region turbulence model
C_P - quantity for positive characteristics used for 1D MOC solution
C_{q1}, C_{q2} - coefficients before q
C_r - courant number
C_{u1}, C_{u2}, C_{u3} - coefficients before u
c - parameter associated with pipe anchor condition
c - superscript denoting values predicted by forward model
c_2 - coefficient used in Daily et al. [39]
$\mathbf{cs}$ - control surface
$\mathbf{cv}$ - control volume
D - diameter of pipe
E - Young's modulus of elasticity of pipe material
E - errors
E^* - merit (error) function
e - thickness of pipe wall
F - wall resistance force
F_{ext} - external forces
f - Darcy-Weisbach friction factor
$\mathbf{g}$ - gravitational acceleration
$\mathbf{H}_m$ - set of measured piezometric head
H - piezometric head
H_A - piezometric head at point A
H_B - piezometric head at point B
H_P - piezometric head at point P
$\mathbf{h}_c$ - set of computed piezometric head
i - index for pipes
J_s - steady friction term
j - index for pipes
K - unsteady resistance coefficient
K_e - effective bulk modulus of elasticity
K_f - bulk modulus of elasticity of the fluid
K_s - steady-state resistance coefficient
K_u - unsteady resistance coefficient and momentum flux of absolute local velocity
k - unsteady friction factor
L - pipe length
l - mixing length
$\mathbf{M}$ - Mach number
m - superscript denoting measured data values
m - time level index
$\mathbf{N}_1$ - set of all pipes with flow toward conjuction node
$\mathbf{N}_2$ - set of all pipes with flow away from conjuction node
N_r - number of computational reaches in radial direction
$\mathbf{n}$ - unit outward normal vector to control surface
n - index of measured series
n - exponential for power law of velocity profile
n_c - number of complete water hammer wave cycles
P - parameter for quasi-steady assumption
P - piezometric pressure
Q - discharge
Q_A - discharge at point A
Q_B - discharge at point B
Q_{ext} - discharge of external flow
Q_P - discharge at point P
q - radial flux
q - flow rate
R, R_* - radius of pipe, dimensionless distance from pipe wall
R - coefficient for MOC formulation
Re - Reynolds number

r - radial coordinate
T - time scale
T_d - time scale for radial diffusion of vorticity
t - time
t' - time used for convolution integral
U_1 - longitudinal velocity scale
$\mathbf{u}$ - unknown vector for subsystem of longitudinal velocity component
u - local longitudinal velocity
u_* - frictional velocity
u' - turbulence perturbation corresponding to u
V - cross-sectional average velocity
$\mathbf{v}$ - velocity vector
$\mathbf{v}$ - unknown vector for subsystem of head and radial velocity component
v - local radial velocity
v' - turbulence perturbation corresponding to v
W - weighting function
X - longitudinal length scale
x - distance along the pipe
y, y_* - distance from pipe wall, dimensionless distance from pipe wall
Z - elevation of pipe centerline from a given datum
$\mathbf{z}$ - unknown vector for system
α - angle between pipe and horizontal direction
α - coefficient in weighting function
β - momentum correction coefficient
β - coefficient in weighting function
γ - unit gravity force
ϵ - distance from the water hammer front
ϵ - eddy viscosity
ϵ - implicit parameter for shear stress
ϵ - implicit parameter for friction
ϵ - measured and modeled data error
ζ - a positive real parameter
η - difference from unity of Coriolis correction
η - constant for weighting function
θ - implicit parameter for radial flux
κ - coefficient for weighting function
κ - coefficient for five-region turbulence model
κ - coefficient for two-layer turbulence model
λ_1 - Lagrangian multiplier
λ_2 - Lagrangian multiplier
ν - kinematic viscosity
ν_p - Poisson ratio
ν_T - total viscosity
ξ - strain
ρ - fluid density
ρ_0 - fluid density at undisturbed state
ρ_e - effective density
σ_1, σ_2 - unknown but desired parameters
σ_x - axial stress
σ_θ - hoop stress
τ - shear stress
τ_w - wall shear stress
τ_{ws} - quasi-steady contribution of wall shear stress
τ_{wu} - discrepancy between unsteady and quasi-steady wall shear stress
ϕ - coefficient in unsteady friction formula

References

[1] Vanderburg, V. H., 1986, "Knowing Technology as if People Mattered," Man-Env. Syst. **16**, pp. 69–75.
[2] Kuhn, T., 1962, *The Structure of Scientific Revolutions*, University of Chicago Press, Chicago, IL.
[3] Menabrea, L. F., 1885, "Note sur les effects de choc de l'eau dans les conduites," C. R. Hebd. Seances Acad. Sci. **47**, July–Dec., pp. 221–224.
[4] Michaud, J., 1878, "Coups de bélier dans les conduites. Étude des moyens employés pour en atteneur les effects," Bull. Soc. Vaudoise Ing. Arch. **4**(3,4), pp. 56–64, 65–77.
[5] Weston, E. B., 1885, "Description of Some Experiments Made on the Providence, RI Water Works to Ascertain the Force of Water Ram in Pipes," Trans. Am. Soc. Civ. Eng. **14**, p. 238.
[6] Carpenter, R. C., 1893, "Experiments on Waterhammer," Trans. ASME, **15**.
[7] Frizell, J. P., 1898, "Pressures Resulting from Changes of Velocity of Water in Pipes," Trans. Am. Soc. Civ. Eng. **39**, pp. 1–18.
[8] Joukowski, N. E., 1898, "Memoirs of the Imperial Academy Society of St. Petersburg," **9**(5) (Russian translated by O Simin 1904), Proc. Amer. Water Works Assoc. **24**, pp. 341–424.
[9] Allievi, L., 1903, "Teoria generale del moto perturbato dell'acqu ani tubi in pressione," Ann. Soc. Ing. Arch. Ithaliana (French translation by Allievi (1904, Revue de mécanique).
[10] Allievi, L., 1913, "Teoria del colpo d'ariete," Atti Collegio Ing. Arch. (English translation by Halmos EE 1929), "The Theory of Waterhammer," Trans. ASME.
[11] Courant, R. and Friedrichs, K. O., 1976, *Supersonic Flow and Shock Waves*, Springer-Verlag, New York.
[12] Jaeger, C., 1933, *Theorie Generale du Coup de Belier*, Dunod, Paris.
[13] Jaeger, C., 1956, *Engineering Fluid Mechanics* translated from German by P.O. Wolf, Blackie, London.
[14] Wood, F. M., 1937, "The Application of Heavisides Operational Calculus to the Solution of Problems in Waterhammer," Trans. ASME **59**, pp. 707–713.
[15] Rich, G., 1944, "Waterhammer Analysis by the Laplace-Mellin Transformations," Trans. ASME, pp. 1944–45.
[16] Rich, G., 1951, *Hydraulic Transients*, 1st Edition, McGraw-Hill, New York, 1951 (Dover Reprint).
[17] Parmakian, J., 1955, *Water-Hammer Analysis*. Prentice-Hall Englewood Cliffs, N.J., 1955 (Dover Reprint, 1963).
[18] Streeter, V. L., and Lai, C., 1963, "Waterhammer Analysis Including Fluid Friction," Trans. Am. Soc. Civ. Eng. **128**, pp. 1491–1524.
[19] Streeter, V. L. and Wylie, E. B., 1967, *Hydraulic Transients*, McGraw-Hill, New York.
[20] Chaudhry, M. H., 1987, *Applied Hydraulic Transients*, Van Nostrand Reinhold, New York.
[21] Watters, G. Z., 1984, *Analysis and Control of Unsteady Flow in Pipelines*, Butterworth, Stoneham, Ma.
[22] Wylie, E. B. and Streeter, V. .L 1984, *Fluid Transients*, FEB Press, Ann Arbor.
[23] Wylie, E. B., Streeter, V. L., and Suo, Lisheng, 1993, *Fluid Transient in Systems*, Prentice-Hall, Englewood Cliffs,
[24] Mitra, A. K., and Rouleau W. T., 1985, "Radial and Axial Variations in Transient Pressure Waves Transmitted Through Liquid Transmission Lines," ASME J. Fluids Eng. **107**, pp. 105–111.
[25] Vardy, A. E., and Hwang, K. L., 1991, "A Characteristic Model of Transient Friction in Pipes," J. Hydraul. Res. **29**(5), pp. 669–685.
[26] Ghidaoui, M. S. 2001, "Fundamental Theory of Waterhammer," Special Issue of the Urban Water J. (Special Issue on Transients, Guest Editor: B. W. Karney), **1**(2), pp. 71–83.
[27] Walker, J. S., 1975, "Perturbation Solutions for Steady One-Dimensional Waterhammer Waves," ASME J. Fluids Eng. **6**, pp. 260–262.
[28] Hinze, J. O., 1975, *Turbulence*, McGraw-Hill Classic Textbook Reissue Series, New York.
[29] Bergant, A. and Simpson, A. R., 1994, "Estimating Unsteady Friction in Transient Cavitating Pipe Flow," *Proc. 2nd Int. Conf. on Water Pipeline Systems*, Edinburgh, UK, May 24–26, BHRA Group Conf. Series Publ. No. 110, pp. 3–15.
[30] Axworthy, D. H., Ghidaoui, M. S., and McInnis, D. A., 2000, "Extended Thermodynamics Derivation of Energy Dissipation in Unsteady Pipe Flow," J. Hydraul. Eng. **126**(4), pp. 276–287.
[31] Brunone, B., Karney, B. W., Mecarelli, M., and Ferrante, M., 2000, "Velocity Profiles and Unsteady Pipe Friction in Transient Flow," J. Water Resour. Plan. Manage. **126**(4), pp. 236–244.
[32] Ghidaoui, M. S., and Mansour, S., 2002, "Efficient Treatment of the Vardy-Brown Unsteady Shear in Pipe Transients," J. Hydraul. Eng. **128**(1), pp. 102–112.
[33] Korteweg, D. J., 1878, "Über die fortpflanzungsgeschwidigkeit des schalles in elastischen rohren," Ann. Phys. Chemie **5**(12), pp. 525–542.
[34] Lighthill, J., 1996, *Waves in Fluids*, Cambridge University Press, UK.
[35] Tijsseling, A. S., 1995, "Fluid-Structure Interaction in Liquid-Filled Pipe Systems: A Review," J. Fluids Struct. **10**, pp. 109–146.

[36] Streeter, V. L. and Wylie, E. B., 1985, *Fluid Mechanics* (8th Edition), McGraw Hill New York.

[37] Silva-Araya, W. F., and Chaudhry, M. H., 1997, "Computation of Energy Dissipation in Transient Flow," J. Hydraul. Eng. **123**(2), pp. 108–115.

[38] Pezzinga, G., 1999, "Quasi-2D Model for Unsteady Flow in Pipe Networks," J. Hydraul. Eng. **125**(7), pp. 676–685.

[39] Daily, J. W., Hankey, W. L., Olive, R. W., and Jordaan, J. M., 1956, "Resistance Coefficients for Accelerated and Decelerated Flows Through Smooth Tubes and Orifices," Trans. ASME **78**(July), pp. 1071–1077.

[40] Shuy, E. B., 1996, "Wall Shear Stress in Accelerating and Decelerating Turbulent Pipe Flows," J. Hydraul. Res. **34**(2), pp. 173–183.

[41] Vardy, A. E., and Brown, J. M. B., 1997, "Discussion on Wall Shear Stress in Accelerating and Decelerating Pipe Flow," J. Hydraul. Res. **35**(1), pp. 137–139.

[42] Ghidaoui, M. S., and Kolyshkin, A. A., 2001, "Stability Analysis of Velocity Profiles in Water-Hammer Flows," J. Hydraul. Eng. **127**(6), pp. 499–512.

[43] Carstens, M. R., and Roller, J. E., 1959, "Boundary-Shear Stress in Unsteady Turbulent Pipe Flow," J. Hydraul. Div., Am. Soc. Civ. Eng. **85**(HY2), pp. 67–81.

[44] Pezzinga, G., 2000, "Evaluation of Unsteady Flow Resistances by Quasi-2d or 1d Models," J. Hydraul. Eng. **126**(10), pp. 778–785.

[45] Eichinger, P. and Lein, G., 1992, *The Influence of Friction on Unsteady Pipe Flow, Unsteady Flow and Fluid Transients*, Bettess and Watts (eds), Balkema, Rotterdam, The Netherlands, 41–50.

[46] Ghidaoui, M. S., Mansour, S. G. S., and Zhao, M., 2002, "Applicability of Quasi Steady and Axisymmetric Turbulence Models in Water Hammer," J. Hydraul. Eng. **128**(10), pp. 917–924.

[47] Vardy, A. E. and Brown, J, M., 1996, "On Turbulent, Unsteady, Smooth-Pipe Friction, Pressure Surges and Fluid Transient," BHR Group, London, pp. 289–311.

[48] Brunone, B. and Golia, U. M., 1991, "Some Considerations on Velocity Profiles in Unsteady Pipe Flows," *Proc. Int. Conf. on Enthropy and Energy Dissipation in Water Resources*, Maratea, Italy, pp. 481–487.

[49] Greco, M., 1990, "Some Recent Findings On Column Separation During Water Hammer," *Excerpta*, G.N.I., Padua, Italy, Libreria Progetto, ed., **5**, 261–272.

[50] Brunone, B., Golia, U. M., and Greco, M., 1991, "Some Remarks on the Momentum Equation for Fast Transients," *Proc. Int. Conf. on Hydr. Transients With Water Column Separation*, IAHR, Valencia, Spain, 201–209.

[51] Brunone, B., Golia, U. M., and Greco, M., 1991, "Modelling of Fast Transients by Numerical Methods," *Proc. Int. Conf. on Hydr. Transients With Water Column Separation*, IAHR, Valencia, Spain, 273–280.

[52] Bergant, A., Simpson, A. R., and Vitkovsky, J., 2001, "Developments in Unsteady Pipe Flow Friction Modelling," J. Hydraul. Res. **39**(3), pp. 249–257.

[53] Brunone, B., Golia, U. M., and Greco, M., 1995, "Effects of Two-Dimensionality on Pipe Transients Modeling," J. Hydraul. Eng. **121**(12), pp. 906–912.

[54] Wylie, E. B., 1997, "Frictional Effects in Unsteady Turbulent Pipe Flows," Appl. Mech. Rev. **50**(11), Part 2, pp. S241–S244.

[55] Vitkovsky, J. P., Lambert, M. F., Simpson, A. R., and Bergant, A., 2000, "Advances in Unsteady Friction Modelling in Transient Pipe Flow," *8th Int. Conf. on Pressure Surges*, The Hague, The Netherlands.

[56] Zielke, W., 1968, "Frequency-Dependent Friction in Transient Pipe Flow," ASME J. Basic Eng. **90**(1), pp. 109–115.

[57] Trikha, A. K., 1975, "An Efficient Method for Simulating Frequency-Dependent Friction in Transient Liquid Flow," ASME J. Fluids Eng. **97**(1), pp. 97–105.

[58] Suzuki, K., Taketomi, T., and Sato, S., 1991, "Improving Zielke's Method of Simulating Frequency-Dependent Friction in Laminar Liquid Pipe Flow," ASME J. Fluids Eng. **113**(4), pp. 569–573.

[59] Vardy, A. E., Hwang, K. L., and Brown, J. M. B., 1993, "A Weighting Model of Transient Turbulent Pipe Friction," J. Hydraul. Res. **31**, pp. 533–548.

[60] Vardy, A. E., and Brown, J. M. B., 1995, "Transient, Turbulent, Smooth Pipe Friction," J. Hydraul. Res. **33**, pp. 435–456.

[61] Almeida, A. B. and Koelle, E., 1992, *Fluid Transients in Pipe Networks, Computational Mechanics Publications*, Elsevier, New York.

[62] Lister, M., 1960, The Numerical Solution of Hyperbolic Partial Differential Equations by the Method of Characteristics, A Ralston and HS Wilf (eds), *Numerical Methods for Digital Computers*, Wiley New York, 165–179.

[63] Wiggert, D. C., and Sundquist, M. J., 1977, "Fixed-Grid Characteristics for Pipeline Transients," J. Hydraul. Div., Am. Soc. Civ. Eng. **103**(HY12), pp. 1403–1415.

[64] Goldberg, D. E., and Wylie, E. B., 1983, "Characteristics Method Using Time-Line Interpolations," J. Hydraul. Eng. **109**(5), pp. 670–683.

[65] Lai, C., 1989, "Comprehensive Method of Characteristics Models for Flow Simulation," J. Hydraul. Eng. **114**(9), pp. 1074–1095.

[66] Yang, J. C., and Hsu, E. L., 1990, "Time-Line Interpolation for Solution of the Dispersion Equation," J. Hydraul. Res. **28**(4), pp. 503–523.

[67] Yang, J. C., and Hsu, E. L., 1991, "On the Use of the Reach-Back Characteristics Method of Calculation of Dispersion," Int. J. Numer. Methods Fluids **12**, pp. 225–235.

[68] Bentley, L. R., 1991, Discussion of "On the Use of the Reach-Back Characteristics Method for Calculation of Dispersion," by J. C. Yang, and EL Hsu, Int. J. Numer. Methods Fluids **13**(5), pp. 1205–1206.

[69] Sibertheros, I. A., Holley, E. R., and Branski, J. M., 1991, "Spline Interpolations for Water Hammer Analysis," J. Hydraul. Eng. **117**(10), pp. 1332–1349.

[70] Karney, B. W., and Ghidaoui, M. S., 1997, "Flexible Discretization Algorithm for Fixed Grid MOC in Pipeline Systems," J. Hydraul. Eng. **123**(11), pp. 1004–1011.

[71] Wood, D. J., Dorsch, R. G., and Lightnor, C., 1966, "Wave-Plan Analysis of Unsteady Flow in Closed Conduits," J. Hydraul. Div., Am. Soc. Civ. Eng. **92**(HY12), pp. 83–110.

[72] Wylie, E. B. and Streeter, V. L., 1970, "Network System Transient Calculations by Implicit Method," *45th Annual Meeting of the Society of Petroleum Engineers of AIME*, Houston, Texas October 4–7, paper No. 2963.

[73] Holly, F. M., and Preissmann, A., 1977, "Accurate Calculation of Transport in Two Dimensions," J. Hydraul. Div., Am. Soc. Civ. Eng. **103**(HY11), pp. 1259–1277.

[74] Chaudhry, M. H., and Hussaini, M. Y., 1985, "Second-Order Accurate Explicitly Finite-Difference Schemes for Water Hammer Analysis," ASME J. Fluids Eng. **107**, pp. 523–529.

[75] Toro, E. F., 1997, *Riemann Solvers and Numerical Methods for Fluid Dynamics*, Springer-Verlag, Berlin.

[76] Toro, E. F., 2001, *Shock-Capturing Methods for Free-Surface Shallow Flows*, Wiley Ltd, Chichester, England.

[77] Guinot, V., 2002, "Riemann Solvers for Water Hammer Simulations by Godunov Method," Int. J. Numer. Methods Eng. **49**, pp. 851–870.

[78] Hwang, Y. H., and Chung, N. M., 2002, "A Fast Godunov Method for the Water-Hammer Problem," Int. J. Numer. Methods Fluids **40**, pp. 799–819.

[79] O'Brian, G. G., Hyman, M. A., and Kaplan, S., 1951, "A Study of the Numerical Solution of Partial Differential Equations," J. Math. Phys. **29**(4), pp. 223–251.

[80] Damuller, D. C., Bhallamudi, S. M., and Chaudhry, M. H., 1989, "Modelling Unsteady Flow in Curved Channel," J. Hydraul. Eng. **115**(11), pp. 1471–1495.

[81] Samuels, G. P., and Skeel, P. C., 1990, "Stability Limits for Preissmann's Scheme," J. Hydraul. Div., Am. Soc. Civ. Eng. **116**(HY8), pp. 997–1011.

[82] Karney, B. W., and Ghidaoui, M. S., 1992, "Discussion on Spline Interpolations for Water Hammer Analysis," J. Hydraul. Eng. **118**(11), pp. 1597–1600.

[83] Sivaloganathan, K., 1978, "Flood Routing by Characteristic Methods," J. Hydraul. Div., Am. Soc. Civ. Eng. **107**(HY7), pp. 1075–1091.

[84] Wylie, E. B., 1980, "Inaccuracies in the Characteristics Method," *Proc. Spec. Conf. on Comp. and Physical Modelling in Hydr. Eng.* ASCE, Chicago, 165–176.

[85] Ghidaoui, M. S., and Karney, B. W., 1994, "Equivalent Differential Equations in Fixed-Grid Characteristics Method," J. Hydraul. Eng. **120**(10), pp. 1159–1176.

[86] Ghidaoui, M. S., Karney, B. W., and McInnis, D. A., 1998, "Energy Estimates for Discretization Errors in Waterhammer Problems," J. Hydraul. Eng. **123**(11), pp. 384–393.

[87] Das, D., and Arakeri, J. H., 1998, "Transition of Unsteady Velocity Profiles with Reverse Flow," J. Fluid Mech. **374**, pp. 251–283.

[88] Brunone, B., Karney, B. W., and Ferrante, M., 1999, "Velocity Profiles Unsteady Friction Losses and Transient Modelling," *Proc. 26th Annu. Water Resour. Plng. and Mgmt. Conf.* ASCE, Reston, VA (on CD-ROM).

[89] Lodahl, C. R., Sumer, B. M., and Fredsoe, J., 1998, "Turbulent

Combined Oscillatory Flow and Current in Pipe,'' J. Fluid Mech. **373**, pp. 313–348.

[90] Ghidaoui, M. S., and Kolyshkin, A. A., 2002, ''A Quasi-Steady Approach to the Instability of Time-Dependent Flows in Pipes,'' J. Fluid Mech. **465**, pp. 301–330.

[91] Pezzinga, G., and Scandura, P., 1995, ''Unsteady Flow in Installations with Polymeric Additional Pipe,'' J. Hydraul. Eng. **121**(11), pp. 802–811.

[92] Greenblatt, D., and Moss, E. A., 1999, ''Pipe-Flow Relaminarization by Temporal Acceleration,'' Phys. Fluids **11**(11), pp. 3478–3481.

[93] He, S., and Jackson, J. D, 2000, ''A Study of Turbulence Under Conditions of Transient Flow in a Pipe,'' J. Fluid Mech. **408**, pp. 1–38.

[94] Tu, S. W., and Ramaprian, B. R., 1983, ''Fully Developed Periodic Turbulent Pipe Flow–Part 1: Main Experimental Results and Comparison with Predictions,'' J. Fluid Mech. **137**, pp. 31–58.

[95] Brereton, G. L., Reynolds, W. C., and Jayaraman, R., 1990, ''Response of a Turbulent Boundary Layer to Sinusoidal Free-Stream Unsteadiness,'' J. Fluid Mech. **221**, pp. 131–159.

[96] Akhavan, R., Kamm, R. D., and Shapiro, A. H., 1991, ''Investigation of Transition to Turbulence in Bounded Oscillatory Stokes Flows–Part 1: Experiments,'' J. Fluid Mech. **225**, pp. 395–422.

[97] Akhavan, R., Kamm, R. D., and Shapiro, A. H., 1991, ''Investigation of Transition to Turbulence in Bounded Oscillatory Stokes Flows–Part 2: Numerical Simulations,'' J. Fluid Mech. **225**, pp. 423–444.

[98] Silva-Araya, W. F., and Chaudhry, M. H., 2001, ''Unsteady Friction in Rough Pipes,'' J. Hydraul. Eng. **127**(7), pp. 607–618.

[99] Ohmi, M., Kyomen, S., and Usui, T., 1985, ''Numerical Analysis of Transient Turbulent Flow in a Liquid Line,'' Bull. JSME **28**(239), pp. 799–806.

[100] Wood, D. J., and Funk, J. E., 1970, ''A Boundary-Layer Theory for Transient Viscous Losses in Turbulent Flow,'' ASME J. Basic Eng. **102**, pp. 865–873.

[101] Bratland, O., 1986, ''Frequency-Dependent Friction and Radial Kinetic Energy Variation in Transient Pipe Flow,'' *Proc. 5th Int. Conf. on Pressure Surges*, BHRA, Hannover, Germany, 95–101.

[102] Rodi, W., 1993, *Turbulence Models and Their Application in Hydraulics: A State-of-the-Art Review*, 3rd Edition, Int. Association for Hydraulic Research, Delft, Balkema.

[103] Kita, Y., Adachi, Y., and Hirose, K., 1980, ''Periodically Oscillating Turbulent Flow in a Pipe,'' Bull. JSME **23**(179), pp. 654–664.

[104] Eggels, J. G. M., 1994, ''Direct and Large Eddy Simulation of Turbulent Flow in a Cylindrical Pipe Geometry,'' PhD Dissertation, Delft University of Technology.

[105] Zhao, M., and Ghidaoui, M. S., 2003, ''An Efficient Solution for Quasi-Two-Dimensional Water Hammer Problems,'' J. Hydraul. Eng., **129**(12), pp. 1007–1013.

[106] Karney, B. W., and McInnis, D., 1990, ''Transient Analysis of Water Distribution Systems,'' J. AWWA **82**(7), pp. 62–70.

[107] Wylie, E. B., 1983, ''The Microcomputer and Pipeline Transients,'' J. Hydraul. Div., Am. Soc. Civ. Eng. **109**(HY12), pp. 539–42.

[108] Karney, B. W., 1984, ''Analysis of Fluid Transients in Large Distribution Networks,'' Ph.D. thesis, University of British Columbia, Vancouver, Canada.

[109] Fox, J. A., 1977, *Hydraulic Analysis and Unsteady Flow in Pipe Networks*, MacMillan Press, London.

[110] Koelle, E., 1982, ''Transient Analysis of Pressure Conduit Hydraulic Systems,'' *Proc the Int. Institute on Hydraulic Transients and Cavitation*, Sao Paulo, Brazil, B1.1–B1.38.

[111] McInnis, D. A., 1992, ''Comprehensive Hydraulic Analysis of Complex Pipe Systems,'' Ph.D. thesis, University of Toronto, Toronto, Canada.

[112] McInnis, D. A., Karney, B. W., and Axworthy, D. H., 1997, ''Effi-

cient Valve Representation in Fixed-Grid Characteristics Method,'' J. Hydraul. Eng. **123**(8), pp. 709–718.

[113] Beck, J. L. and Katafygiotis, L. S., 1992, ''Updating Dynamic Models and Their Associated Uncertainties for Structural Systems,'' *Pro. the 9th Engineering Mechanics Conference*, L. D. Lutes and J. M. Niedzwecki, eds., ASCE, Reston, VA, pp. 681–684.

[114] Sykes, J. F., 1985, ''Sensitivity Analysis for Steady State Ground Water Flow Using Adjoint Operators,'' Water Resour. Res. **21**(3), pp. 359–371.

[115] Sun, N. Z., and Yeh, W. G., 1990, ''Coupled Inverse Problems in Groundwater Modeling–2: Identifiability and Experimental Design,'' Water Resour. Res. **26**(10), pp. 2527–2540.

[116] Sun, N. Z., 1994, *Inverse Problems in Groundwater Modeling*, Kluwer Academic Publishers.

[117] Jarny, Y., Ozisik, M. N., and Bardon, J. P., 1991, ''A General Optimization Method Using Adjoint Equation for Solving Multidimensional Inverse Heat Conduction,'' Int. J. Heat Mass Transfer **34**(11), pp. 2911–2919.

[118] Cacuci, D. G., and Hall, M. C. G., 1984, ''Efficient Estimation of Feedback Effects with Application to Climate Models,'' J. Atmos. Sci. **13**(2), pp. 2063–2068.

[119] Hall, M. C. G. , 1986, ''Application of Adjoint Sensitivity Theory to an Atmospheric General Circulation Model,'' J. Atmos. Sci. **43**(22), pp. 2644–2651.

[120] Marchuk, G. I., 1995, *Adjoint Equations and Analysis of Complex Systems*, Kluwer, London.

[121] Liggett, J. A., and Chen, L. C., 1994, ''Inverse Transient Analysis in Pipe Networks,'' J. Hydraul. Eng. **120**(8), pp. 934–995.

[122] Karney, B. W. and Tang, K., 2003, personal communication.

[123] Brunone, B., 1999, ''Transient Test-Based Technique for Leak Detection in Outfall Pipes,'' J. Water Resour. Plan. Manage. **125**(5), pp. 302–306.

[124] Brunone, B., and Ferrante, M., 2001, ''Detecting Leaks in Pressurised Pipes by Means of Transient,'' J. Hydraul. Res. **39**(5), pp. 539–547.

[125] Mpesha, W., Gassman, S. L., and Chaudhry, M. H., 2001, ''Leak Detection in Pipes by Frequency Response Method,'' J. Hydraul. Eng. **127**(2), pp. 137–147.

[126] Mpesha, W., Chaudhry, M. H., and Gassman SL 2002, ''Leak Detection in Pipes by Frequency Response Method Using a Step Excitation,'' J. Hydraul. Res. **40**(1), pp. 55–62.

[127] Ferrante, M., and Brunone, B., 2002, ''Pipe System Diagnosis and Leak Detection by Unsteady-State Tests–1: Harmonic Analysis,'' Adv. Water Resour. **26**, pp. 95–105.

[128] Wang, Xiao-Jian, Lambert, M. F., Simpson, A. R., and Liggett, J. A., 2002, ''Leak Detection in Pipelines Using the Damping of Fluid Transients,'' J. Hydraul. Eng. **128**(7), pp. 697–711.

[129] Ferrante, M., and Brunone, B., 2002, ''Pipe System Diagnosis and Leak Detection by Unsteady-State Tests–2: Wavelent Analysis,'' Adv. Water Resour. **26**, pp. 107–116.

[130] Payment, P., 1999, ''Poor Efficacy of Residual Chlorine Disinfectant in Drinking Water to Inactivate Waterborne Pathogens in Distribution system,'' Can. J. Microbiol. **45**(8), pp. 709–715.

[131] Funk, J. E., van Vuuren, S. J., Wood, D. J., and LeChevallier, M., 1999, ''Pathogen Intrusion into Water Distribution Systems Due to Transients,'' *Proc. 3rd ASME/JSME Joint Fluids Engineering Conf.*, July 18–23, San Francisco, California.

[132] Germanopoulos, G. and Jowitt, P. W., 1989, ''Leakge Reduction by Excessive Pressure Minimization in a Water Supply Network,'' *Proc. Inst. of Civ. Eng.* (UK), 195–214.

[133] McInnis, D. A., 2003, ''A Relative-Risk Assessment Framework for Evaluating Pathogen Intrusion During Transient Events in Water Pipelines,'' *Urban Water J.* (Special Issue on Transients, Guest Editor: B. W. Karney), **1**(2), pp. 113–127.

Mohamed Ghidaoui received his B.A.Sc., M.A.Sc. and Ph.D. all in Civil Engineering from the University of Toronto, Canada, in 1989, 1991, and 1993, respectively. Since July 1993, he has been with the Department of Civil Engineering at the Hong Kong University of Science and Technology (HKUST) where he is an Associate Professor. His research interests include modeling of surface water flows and water hammer: unsteady friction in conduits, turbulence modeling of fast transients, flow stability of time-dependent flows and turbulent shallow shear flow, numerical modeling of surface and closed conduit flows, and application of Bolzmann theory in hydraulics. He is a member of the International Association of Hydraulic Research (IAHR) and the American Society of Civil Engineers (ASCE). He is a founding member of IAHR-Hong Kong and currently serves as its president. He is an Associate Editor of the Journal of Hydraulic Research and an advisory board member of the Journal of Hydroinformatics. His awards include the Albert Berry Memorial Award, American Water Works Association; runner-up for the Hilgard Award for best paper, Journal of Hydraulic Engineering; and Teaching Excellence Awards, School of Engineering, HKUST.

Ming Zhao obtained his Ph.D. in April 2004 from the Department of Civil Engineering, at Hong Kong University of Science and Technolgy. He obtained both his B.A.Eng. in hydraulic engineering and B.A.Sc. in eneterprise management in 1999 from Tsinghua University. His research interests include numerical simulation of unsteady pipe flows, open channel flows, turbulence modeling in hydraulics, and stability analysis for fluid flows.

David H. Axworthy is a registered professional engineer with a consulting engineering firm in Los Angeles, California. He obtained his B.A.Sc. (1991), M.A.Sc. (1993) and Ph.D. (1997) in civil engineering from the University of Toronto. Axworthy has analyzed pressure transients created by the operation of pump stations and valves and designed surge protection for water supply, wastewater, fire protection, deicing, diesel, and jet fuel systems. A member of the ASCE and AWWA, Axworthy is coauthor of a water hammer analysis model (TransAM), serves as a reviewer for the ASME Journal of Fluids Engineering, and has published scientific papers in the area of pipe network transients.
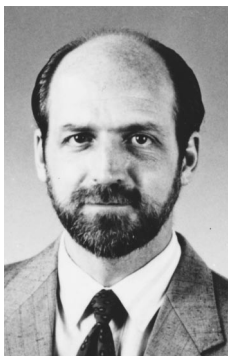
Duncan A. McInnis (Ph.D., P.Eng., MHKIE) has degrees in environmental biology and civil engineering. He has 20 years of scientific and professional engineering experience in computational hydraulics, simulation, and computer modeling of surface water and pipeline systems. McInnis has been a Lecturer of Civil Engineering and Senior Project Manager at the Hong Kong University of Science and Technology. He is currently the Manager of Water Resources with Komex International Ltd., an international environmental consulting firm.